Ecological, morphological and molecular characterization of Kryptoperidinium sp. (Dinophyceae) from two Mediterranean coastal shallow lagoons

Harmful Algae

Ecological, morphological and molecular characterization of Kryptoperidinium sp. (Dinophyceae) from two Mediterranean coastal shallow lagoons.

--Manuscript Draft--

Manuscript Number:	HARALG-D-20-00022R1
Article Type:	Research Paper
Keywords:	Kryptoperidinium; blooms; LSU; ITS; SSU; endosymbiont
Corresponding Author:	Silvia Pulina University of Cagliari Cagliari, ITALY
First Author:	Cecilia T Satta
Order of Authors:	Cecilia T Satta
	Silvia Pulina
	Albert Reñé
	Bachisio M Padedda
	Tiziana Caddeo
	Nicola Fois
	Antonella Lugliè
Abstract:	In this study, the field ecology of Kryptoperidinium sp. was examined in two Mediterranean shallow lagoons, Calich (CA) and Santa Giusta (SG) in Sardinia, Italy. Kryptoperidinium cell density and the environmental conditions were examined monthly from 2008 to 2015 in CA and from 2011 to 2016 in SG. Cell morphology was determined by observing specimens taken from the field and from cultures that were established by single-cell isolation from samples collected in the two lagoons. The molecular identity of strains from each lagoon was also ascertained. The growth rates of the strains were determined under three different temperature conditions and six salinity treatments. The two wild populations shared the same morphology and the cultured strains were morphologically and molecularly identical. The SSU and 5.8S phylogenies show the presence of two clusters within the available Kryptoperidinium sequences and the strains obtained in this study clustered with others from the Mediterranean and Baltic. The multiannual dynamics of Kryptoperidinium sp. in the field significantly differed in the two lagoons, showing much higher cell densities in CA than in SG. The presence of Kryptoperidinium sp. was detected throughout the year in CA, with recurrent blooms also affecting the adjacent coastal area. In contrast, Kryptoperidinium sp. was sporadically observed in SG. The variation in the environmental parameters was fairly wide during the presence and blooms of Kryptoperidinium sp., especially in CA. The application of Generalized Linear Models to the field data revealed a significant role of rainfall and dissolved inorganic nitrogen on the presence and blooms of the species. Although growth rates were similar between the two strains, significant differences were detected for the 10 and 40 salinity treatments. The results obtained in this study add to our knowledge about the ecology of a harmful species that is not well understood in transitional ecosystems such as Mediterranean lagoons.

Highlights:

- Ecological plasticity of *Kryptoperidinium* was confirmed in Mediterranean lagoons
- Different behavior of *Kryptoperidinium* was detected in two Mediterranean lagoons
- *Kryptoperidinium* blooms impacted tourist and recreational use of nearby coastal areas

Ecological, morphological and molecular characterization of *Kryptoperidinium* sp. (Dinophyceae) from two Mediterranean coastal shallow lagoons.

Cecilia Teodora Satta[1,2], Silvia Pulina[2]*, Albert Reñé[3], Bachisio Mario Padedda[2], Tiziana Caddeo[2], Nicola Fois[1], Antonella Lugliè[2]

[1]Agris Sardegna, S.S. 291 Sassari-Fertilia km 18 600, Bonassai (Olmedo), Sardinia, Italy
[2] Università di Sassari, Dipartimento di Architettura, Design e Urbanistica, Via Piandanna 4, Sassari, Sardinia, Italy;
[3] Institut de Ciències del Mar (CSIC), Dpt. Biologia Marina i Oceanografia, Passeig Marítim de la Barceloneta 37−49, Barcelona, Catalonia, Spain

*Corresponding author: Silvia Pulina, email: pulinasi@uniss.it

Abstract

In this study, the field ecology of *Kryptoperidinium* sp. was examined in two Mediterranean shallow lagoons, Calich (CA) and Santa Giusta (SG) in Sardinia, Italy. *Kryptoperidinium* cell density and the environmental conditions were examined monthly from 2008 to 2015 in CA and from 2011 to 2016 in SG. Cell morphology was determined by observing specimens taken from the field and from cultures that were established by single-cell isolation from samples collected in the two lagoons. The molecular identity of strains from each lagoon was also ascertained. The growth rates of the strains were determined under three different temperature conditions and six salinity treatments. The two wild populations shared the same morphology and the cultured strains were morphologically and molecularly identical. The SSU and 5.8S phylogenies show the presence of two clusters within the available *Kryptoperidinium* sequences and the strains obtained in this study clustered with others from the Mediterranean and Baltic. The multiannual dynamics of *Kryptoperidinium* sp. in the field significantly differed in the two lagoons, showing much higher cell densities in CA than in SG. The presence of *Kryptoperidinium* sp. was detected throughout the year in CA, with recurrent blooms also affecting the adjacent coastal area. In contrast, *Kryptoperidinium* sp. was sporadically observed in SG. The variation in the environmental parameters was fairly wide during the presence and blooms of *Kryptoperidinium* sp., especially in CA. The application of Generalized Linear Models to the field data revealed a significant role of rainfall and dissolved inorganic nitrogen on the presence and blooms of the species. Although growth rates were similar between the two strains, significant differences were detected for the 10

and 40 salinity treatments. The results obtained in this study add to our knowledge about the ecology of a harmful species that is not well understood in transitional ecosystems such as Mediterranean lagoons.

Keywords: *Kryptoperidinium*; blooms; LSU; ITS; SSU; endosymbiont

1. Introduction

The genus *Kryptoperidinium* belongs to a dinoflagellates Family, the Kryptoperidiniaceae (Pienaar et al., 2007; Takano et al., 2008; Gottschling and McLean, 2013; Janouškovec et al., 2017; Price and Bhattacharya, 2017; Kretschmann et al., 2018) which host a tertiary endosymbiont derived from a diatom (Dodge, 1971). The taxonomic history of *Kryptoperidinium* is intricate. Stein described the type species *K. foliaceum* (Stein) Lindemann as *Glenodinium foliaceum* from the Baltic Sea in 1883. After Stein's initial record, this species was repeatedly revised, reclassified and assigned to different genera such as *Kryptoperidinium*, *Peridinium* and, once again, to *Glenodinium* (e.g., Paulsen, 1908; Lindemann, 1924; Lebour, 1925; Schiller, 1937; Biecheler, 1952; Prager, 1963; Dodge and Crawford, 1969). Further complications with the *Kryptoperidinium* nomenclature emerged recently (Gottschling et al., 2018, 2019). In addition to the repeated taxonomic revisions and the nomenclature issues, the number of species is under review. The presence of a single species within the genus was widely accepted until the morphological and molecular data collected by Kempton et al. (2002) highlighted the possible existence of different species within the genus. Kretschmann et al. (2018) corroborated this conclusion, confirming the presence of at least two clades within the genus *Kryptoperidinium*.

Kryptoperidinium species are usually recorded in transitional ecosystems such as lagoons, estuaries, and tidal creeks (e.g., Jenkinson, 1990; Trigueros et al., 2000; Kempton et al., 2002; Wolny et al., 2004; Lopez-Flores et al., 2006; Figueroa et al., 2009). The species shows a strong euryhaline tolerance whereby it can occur in conditions ranging from almost freshwater (Domingues et al., 2011) to hypersaline water (Saburova et al., 2012). Some populations are listed as high-biomass bloom producer species (Kempton et al., 2002; Wolny et al., 2004; Saburova et al., 2012). The production of toxic compounds by *Kryptoperidinium* species has not been demonstrated yet but blooms can harm both biota and ecosystem functions. Shellfish and fish mortality events were reported during *Kryptoperidinium* blooms in South Carolina estuaries (Lewitus et al., 2003; Wolny et al., 2004) and in Tunisian coastal waters (Turki et al., 2007).

Given their widespread distribution and the ability to give rise to harmful blooms, the field ecology of *Kryptoperidinium* has been fairly well investigated, especially in estuarine waters (Jenkinson,

1990; Trigueros et al., 2000; Wolny et al., 2004). However, less research has been conducted in transitional ecosystems such as Mediterranean coastal lagoons (Lopez-Flores et al., 2006; Turki et al., 2007). Coastal lagoons are key ecosystems that support unique biological communities. These ecosystems play a role in biogeochemical processes and they provide valuable ecosystem services such as food, hydrological balance, climate regulation, flood protection, water purification, and oxygen production (Newton et al., 2018 and references therein). In addition, coastal lagoons are very important areas for human activities and associated economic interests such as fisheries and aquaculture, or recreational and tourist uses (Newton et al., 2014). However, coastal lagoons are very sensitive ecosystems that are experiencing increasing levels of adverse stressors, including climate change, colonization by alien species, eutrophication, and increases in harmful phytoplankton species (Newton et al., 2018 and references therein).

Cells belonging to the *Kryptoperidinium* genus have been frequently observed in Sardinian ecosystems in the Mediterranean, especially in coastal lagoons. In particular, Calich Lagoon (north western coast) has suffered recurrent *Kryptoperidinium* blooms. Conversely, blooms have only been sporadically observed in Santa Giusta Lagoon (central western coast). The different behavior of the *Kryptoperidinium* populations in these two transitional ecosystems located in the same geographical area suggests at least two hypothesis: a) the presence of a strong environmental variation between the two lagoons which results in significant differences in the ecological responses of the species, and/or b) the presence of two different taxa with differing ecological behavior. Accordingly, in this study *Kryptoperidinium* specimens from the two lagoons were characterized morphologically and molecularly and the environmental factors supporting their development in the field were investigated. In addition, the ecology of *Kryptoperidinium* strains from the two lagoons was investigated in culture to determine their exponential growth rates under different temperatures and salinity conditions. In addition to the average conditions found in the lagoons, rare or out-of-range conditions of temperature and salinity were also tested to obtain broad-spectrum information.

2. Material and methods

2.1 Study areas and sampling strategy

Calich (CA) and Santa Giusta (SG) lagoons are located along the western coast of Sardinia, in the northern and central parts, respectively (Fig. 1). They are about 120 km from each other. CA is elongated in shape and its area and average depth are 0.87 km^2 and 1.2 m, respectively. Its catchment basin covers about 432 km^2. One channel permanently connects the lagoon to the sea. A tourist harbor (Fertilia) is located at the mouth of the channel on the western side. There is also a highly frequented beach on the eastern side. SG is circular in shape, with an area of 8.02 km^2 and an

average depth of 1 m. Its catchment basin covers about 137 km^2. There is a permanent connection with the sea through the Pesaria Channel. SG is one of the Marine Ecosystems of Sardinia research sites for the Italian Long-Term Ecological Research network (www.lteritalia.it; https://deims.org/6f7581f0-e663-4681-bf9d-4668d6c3f2ba).

Freshwater inputs derive from three watercourses in CA and from two watercourses in SG (Fig. 1). In both lagoons, the streams have a torrential character, typical of the Mediterranean basin, and the freshwater inputs are mainly driven by rain events. The annual water inflows are 31.5 Mm^3 in CA and 7.8 Mm^3 in SG (B.M. Padedda, unpublished data). Further freshwater inputs (volume data are not available) in CA derive from an urban wastewater treatment plant that has been active since 2009 and from agricultural activities in the catchment (Padedda et al., 2019). In contrast, a diversion system for wastewater has existed at SG since 1995 (Sechi et al., 2001), which ensures the removal of this type of freshwater inputs. Further information on the study areas is reported in Bazzoni et al. (2013), Satta et al. (2014), Pulina et al. (2017), Satta et al. (2017) and Pulina et al. (2018).

The data analyzed in this study was derived from biweekly/monthly sampling conducted from May 2011 to September 2016 in SG and from September 2008 to June 2015 in CA. The details of the sampling scheme are shown in Supplementary Tables 1 and 2. Samples were collected between 10:00 a.m. and 1:00 p.m. from four sampling stations in SG (1SG, 2SG, 3SG, 4SG) and three in CA (1CA, 2CA, 3CA) (Fig. 1). Major interruptions of sampling occurred from December 2012 to May 2013 in SG and from June 2012 to May 2014 in CA (Supplementary Tables 1 and 2). Occasionally partial sampling was carried out (i.e., at fewer sampling stations) or sampling was not carried out at all due to adverse weather and climatic conditions (Supplementary Tables 1 and 2).

2.2 Field sample collection and processing

2.2.1 Field measurements

Water temperature (Temp) and salinity (Sal) were measured *in situ* using Idronaut (Idronaut Srl, Brugherio, Italy) and YSI 6600 v2 (YSI Inc., Yellow Springs, USA) multiparameter probes. Daily rainfall (Rain) data from 2011 to 2016 (for SG) and from 2008 to 2015 (for CA) were obtained from Servizio Metereologico Aeronautica Militare for CA and from the Dipartimento Specialistico Regionale Idrometeoclimatico (SAR) for SG.

2.2.2 Phytoplankton samples

Samples for phytoplankton analyses were collected at about 30 cm depth. In each sampling, one sample was immediately fixed in 1% Lugol's iodine solution and a second sample was kept alive. Cell density on the fixed sample was determined following Utermöhl (1958). Cell counts (300 cells per sample, when possible) were made under an Axiovert 25 inverted microscope (Carl Zeiss,

Oberkochen, Germany) at 200x magnification within 2 weeks after sampling. Species identification was based on the observation of the cell shape and swimming behavior of living material and on the thecal plate tabulation of fixed cells stained with Calcofluor white (Fritz and Triemer, 1985).

2.2.3 Nutrient samples

Samples for nutrient analyses were collected at about 30 cm depth. Nutrient samples were analyzed within a few hours after the sampling. Concentrations of inorganic nutrients such as reactive phosphorus (PO_4), ammonium (NH_4), nitrate (NO_3), and nitrite (NO_2), were determined in the filtered samples according to the methods of Strickland and Parsons (1972). Total dissolved inorganic nitrogen (DIN) was calculated as the sum of NH_4, NO_3, and NO_2.

2.3 Origin of strains and morphological characterization

Kryptoperidinium strains (KryCA_Uniss and KrySG_Uniss) were obtained by single-cell isolation in April 2014 and August 2015 from CA and SG, respectively. The strains were cultured at a temperature of 20 °C ±1 °C with an approximate illumination of 100 µmol photons m^{-2} s^{-1} and a photoperiod of 12:12 h light:dark (L:D). The cells were grown and maintained in L1 medium (Guillard and Hargraves, 1993) without added silica. The medium was prepared with filtered aged seawater from an oligotrophic Sardinian coastal area and adjusted to a salinity of 30 (KrySG_Uniss) and 20 (KryCA_Uniss) by the addition of sterile distilled water, based on the mean salinity of the source lagoon.

The morphology of living and fixed cells from cultures and from the field was determined using Axiovert 100 and Axiovert 10 (Carl Zeiss, Oberkochen, Germany) inverted microscopes equipped with epifluorescence and differential interference contrast optics. Light microscopic examination of the thecal plate tabulation was performed on fixed cells (Lugol's iodine, 1% final concentration) stained with Calcofluor white (Fritz and Triemer, 1985). Chloroplast autofluorescence was examined in live cells. The shape and location of the nucleus was determined after staining 2% formalin-fixed cells for 10 min with 4'-6-diamidino-2-phenylindole (DAPI). Photographs were taken with a Zeiss Axiocam (Carl Zeiss, Oberkochen, Germany; Axiovert 100) and a Spot Flex digital camera (Spot Imaging, Sterling Heights, Michigan, USA; Axiovert 10). Cell size was determined from cultured and wild fixed material at 400x magnification using a calibrated eyepiece micrometer.

2.4 Molecular and phylogenetic analyses

Genomic DNA from KrySG_Uniss and KryCA_Uniss strains was extracted from ~15 mL of exponentially growing cultures. The cells were harvested by centrifugation at 300 *x g* for 15 min. The pellet was transferred to a 2-mL microcentrifuge tube and centrifuged at 6,000 *x g* for 5 min. Total genomic DNA was extracted from the final pellet using a DNeasy Blood and Tissue kit (Qiagen), following the manufacturer's instructions.

The ribosomal DNA from the SSU, LSU, and ITS regions was amplified. For both SSU and LSU rDNA, a first PCR was conducted in order to amplify the region of interest, and subsequent nested PCRs were performed to obtain the dinoflagellate SSU rDNA, the endosymbiont SSU rDNA, and the dinoflagellate LSU rDNA sequences. All PCR amplifications were done in a 50 µL mixture containing 1 µL of the extracted template DNA, 5 µL of 10X buffer, 1.5 µL of $MgCl_2$, and 0.25 µL of Hot Start Taq DNA polymerase (Biotechrabbit, Hennigsdorf, Germany), 1 µL of dNTP 0.2 mM each (Qiagen) and 0.4 mM of each primer. For SSU rDNA, the combination of the primers EukA and EukB (Medlin et al., 1988) was first used. The PCR amplification parameters consisted of 5 min at 94 °C, followed by 35 cycles of 1 min at 94 °C, 90 sec at 55 °C, 2 min at 72 °C, ending with a final hold of 7 min at 72 °C. The resulting PCR product was used as template for subsequent reactions. The primers Dino18SF1 and 18ScomR1 (Lin et al., 2006; Zhang and Lin, 2005) were used for the dinoflagellate nested PCR, consisting of 5 min at 94 °C, followed by 30 cycles of 45 sec at 94 °C, 1 min at 55 °C, 3 min at 72 °C, ending with a final hold of 10 min at 72 °C. The primers DiaF and DiaR (Zhang et al., 2011) were used for the endosymbiont nested PCR, with the same PCR amplification parameters as the SSU amplification. The primers D1R and D2C (Scholin et al., 1994) were used to amplify the D1/D2 domains of the LSU rDNA, and for the dinoflagellate nested PCR the primers DinFi and DinRi (Logares et al., 2007) were used. The LSU PCR started with 5 min at 94 °C, followed by 40 cycles of 20 sec at 95 °C, 30 sec at 55 °C, 1 min at 72 °C, ending with a final hold of 10 min at 72 °C. The PCR amplification parameters for the dinoflagellate nested LSU PCR were equivalent to the SSU except for the annealing temperature of 52 °C for 1 min. The primers ITSA and ITSB (Adachi et al., 1994) were used to amplify the ITS region. The ITS PCR started with 5 min at 94 °C, followed by 35 cycles of 20 sec at 94 °C, 10 sec at 57 °C, 50 sec at 70 °C, ending with a final hold of 5 min at 70 °C.

An aliquot of the final PCR products was electrophoresed through a 1.2% agarose gel and the remainder was frozen at −20 °C until sequenced. Purification and sequencing were carried out by an external service (Genoscreen, Lille, France) using a 3730XL DNA sequencer. The GenBank Accession numbers are: MN963957–MN963960 and MN963988–MN963989 (Supplementary Table 3). The GenBank Accession number for the endosymbiont sequence is MN963987.

The sequences generated in this study were aligned with sequences obtained from GenBank belonging to the genus *Kryptoperidinium*, Kryptoperidiniaceae representatives, and other dinoflagellate species used as outgroups (see Supplementary Table 3). The phylogenies of the three sequenced rDNA regions were constructed, as well as a concatenated phylogeny of the SSU, 5.8S-ITS, and LSU rDNA. The dataset for each region was aligned separately using MAFFT v. 7 (Katoh et al., 2002). For the concatenated phylogeny, only representatives with at least two of the rDNA regions available were used. Poorly aligned positions and divergent regions were removed using Gblocks v. 0.91b (Castresana, 2000). Alignments and concatenation were manually verified using Geneious v. R6. The GTR model with a GAMMA distribution was selected for all datasets. Phylogenetic analyses were performed using maximum likelihood (ML) and Bayesian approaches. For the ML tree, the MPI version of RAxML (Randomized Axelerated Maximum Likelihood) v. 8.2.3 (Stamatakis, 2014) was used. The most likely tree was established from 1,000 searches. The ML bootstrap support (BS) was analyzed with 1,000 replicates. The Bayesian analysis was carried out with MrBayes v. 3.2 (Ronquist et al., 2012) using the same evolutionary model. The consensus tree was obtained from post burn-in trees. Statistical support values for ML BS, and Bayesian posterior probabilities (BPP), as determined from the ML analyses, are reported for the tree topology.

2.5 Growth experiments

Growth experiments were carried out at three temperatures (11 °C, 20 °C, 30 °C) in combination with six salinities (5, 10, 20, 30, 40, 50) using a growth cabinet for each temperature. Temperatures of 11 °C and 20 °C were selected since they represent the mean temperature in winter and the temperature annual mean in the two lagoons, respectively. The temperature of 30 °C was selected since it represents the maximum temperature in summer in the two lagoons. The six salinities were selected since they correspond to: (A) from 5 to 30: range of salinity variation in CA; (B) from 20 to 40: range of salinity variation in SG; (C) 50: out of range value. The salinities below 30 were obtained by diluting aged seawater from an oligotrophic Sardinian coastal area with distilled water, whereas salinities of 40 and 50 were obtained through evaporation with mild heating. Nutrients, trace metals, and vitamins of the L1 medium (Guillard and Hargraves, 1993) were added after the salinity was adjusted. Cultures of the two strains were pre-adapted to experimental conditions through stepwise transfer of stock cultures to each temperature and salinity regime for about two months.

Acclimated stock cultures were inoculated into triplicate polypropylene flasks filled with 50 mL of each salinity-adjusted media. Flasks were inoculated with 500 cells of each stock culture mL^{-1}, and

1 mL was sampled every 2 days for 1 month. The 1 mL subsamples were fixed with Lugol's solution for cell enumeration in Sedgewick-Rafter chambers; at least 200 cells were counted at 200x magnification under an Axiovert 25 inverted microscope. The cell abundances obtained in the growth experiments were used to determine the exponential growth rates (r) according to Guillard (1973). The growth rate for each flask culture was estimated using data from different days (at least three points) depending on the start and duration of the respective exponential phase.

2.6 Statistical analyses

One-way analysis of variance (ANOVA) was performed to ascertain if there were any significant differences in environmental conditions (Temp, Sal, and nutrients) and in *Kryptoperidinium* cell densities among the sampling stations of each lagoon and between the two lagoons. ANOVA was also conducted on the Rain data to test for any significant difference between the two lagoons. Rain data were obtained by summing daily rainfall values to get monthly accumulations. Monthly rain accumulation data was averaged over the years. Prior to ANOVA, normal distribution (Kolmogorov-Smirnov test) and homogeneity of variance (Bartlett test) were verified. For PO_4 and DIN data the Welch correction was applied (data with non-homogeneous variance). DIN data were square root transformed. For cell density the Kruskal-Wallis test (not normally distributed data) was applied after the $\log_{10}$ (x+1) transformation of data. ANOVAs were also used to verify any significant difference in cell length and width between field and culture data within and between strains. Three-way ANOVA was applied to verify significant differences in the growth rates of *Kryptoperidinium* between SG and CA cultured strains and at the different temperatures and salinities. Interactions between *Kryptoperidinium* data and the environmental variables were analyzed using Generalized Linear Models (GLMs). *Kryptoperidinium* observations in field samples were transformed to binary data (presence/absence). Consequently, the logit-link function for binomial distribution was applied (McCullagh and Nelder, 1989). In addition to the basic presence/absence dataset, two different thresholds of *Kryptoperidinium* cell densities were also considered, the first considering as presence all the records $>2 \times 10^5$ cells L^{-1} and the second considering all the records $>3 \times 10^5$ cells L^{-1}. The three series of models were applied separately to the CA and SG datasets, and on the entire set of data (CA plus SG data). The fixed terms (predictor variables) of the GLMs were Sal, Rain, PO_4, and DIN. Analyses were performed in the statistical and programming software R 3.2.1 (R Development Core Team, 2014).

3. Results

3.1 *Kryptoperidinium* sp. dynamics and relationship with environmental variables

ANOVA revealed no significant differences among the sampling stations in both lagoons for any of the environmental variables or for *Kryptoperidinium* sp. cell density (data not shown). Therefore, all data were grouped by months to reconstruct the monthly mean dynamics of each variable in the two lagoons.

Mean monthly Temp varied within a similar range in the two lagoons (Fig. 2). Annual means were 19.22 °C and 19.27 °C in SG and CA, respectively. No significant differences were detected for Temp between the lagoons. Monthly means of Sal were higher in SG and varied over a wider range in CA (Fig. 2). Annual means were 32.13 in SG and 17.73 in CA. Sal data differed significantly between the two lagoons ($F = 24.51$, $p < 0.001$). Monthly means of accumulated Rain were higher and varied over a wider range in CA than in SG (Fig. 2). Annual means were 504.40 mm and 1001.46 mm in SG and CA, respectively. Rain data differed significantly between the two lagoons ($F = 7.89$, $p < 0.05$). Monthly mean values for inorganic nutrients (DIN and PO_4) and their ratio (DIN:PO_4) were higher in CA than in SG (Fig. 3). DIN, PO_4, and DIN:PO_4 differed significantly between the two lagoons (DIN: $F = 24.04$, $p < 0.001$; PO_4: $F = 25.40$, $p < 0.001$; DIN:PO_4: $F = 11.50$, $p < 0.01$).

During the study period, *Kryptoperidinium* sp. was detected in all months except September in CA. However in SG, it was only found in February, July and August (Fig. 4, Table 1). The monthly means for cell density were higher in CA than in SG, with maximum values of 57.21×10^4 cells L^{-1} in April in CA and 5.29×10^4 cells L^{-1} in July in SG (Table 1). The maximum cell densities were notably higher in CA than in SG, ranging from 1.04×10^4 cells L^{-1} (in October) to 422.51×10^4 cells L^{-1} (in April) in CA and from 0.12×10^4 cells L^{-1} (in February) to 63.54×10^4 cells L^{-1} (in July) in SG (Table 1). *Kryptoperidinium* cell density differed significantly between the two lagoons ($\chi_2 = 12.29$, $p < 0.001$). Recurrent discolorations of the water were observed when cell densities were higher than $2–3 \times 10^5$ cells L^{-1} in CA. Blooms were frequently also detected along the adjacent coastal areas in association with discoloration events in the lagoon, especially in summer (July). Samples taken in these coastal areas confirmed the presence of the species (data not shown). The highest *Kryptoperidinium* cell densities in SG coincided with the highest monthly means for Temp (27.4 ± 1.9°C) and Sal (37.0 ± 1.3), and the lowest values for Rain (7.6 ± 7.8 mm) (Fig. 4). In contrast, the species was recorded over a wider range of Temp, Sal, and Rain monthly mean values in CA (Fig. 4). The highest maximum density values in CA were observed in well identified periods in spring (March-April) and summer (July) (Fig. 4, Table 1). In the spring months, the monthly means of Temp were 13.6 ± 4.2 °C in March and 19.4 ± 3.6 °C in April and the monthly means of Sal were 15.9 ± 7.0 in March and 15.8 ± 5.8 in April. Monthly means of Rain were 96.5 ± 41.0 mm in March and 86.1 ± 34.5 mm in April. In July, the highest cell densities coincided with the highest

monthly means of Temp and Sal, equal to 27.3 ± 1.5 °C and to 26.1 ± 2.7, respectively (Fig. 4). Monthly mean Rain corresponded to the lowest values recorded, at 11.8 ± 14.0 mm (Fig. 4).

In SG, *Kryptoperidinium* detections coincided with intermediate to high monthly means of DIN and low PO_4 concentrations (Fig. 5; Table 2). The highest *Kryptoperidinium* cell densities in SG (July) coincided with a DIN range of 4.30-31.34 µM and a PO_4 range of 0.15-0.29 µM. Monthly mean concentrations of the same nutrients were more variable in CA when *Kryptoperidinium* was detected (Fig. 5; Table 2). During spring blooms (March-April) in CA, DIN and PO_4 concentrations ranged from 42.5 µM to 123.97 µM and from 0.30 µM to 8.09 µM, respectively. During summer blooms (July), DIN and PO_4 concentrations were generally lower, ranging from 2.43 µM to 2.50 µM and from 0.32 µM to 0.58 µM, respectively.

The GLMs showed that DIN and Rain had significant effects on the presence of *Kryptoperidinium* in CA (Table 3). No significant relationships were detected with cell density $>2 \times 10^5$ cells L^{-1} and $>3 \times 10^5$ cells L^{-1} (data not shown). The strong collinearity among data forced the elimination of PO_4 in the application of the GLM on the SG dataset and on the entire set of data (CA plus SG data). Results showed that DIN significantly influenced the presence of *Kryptoperidinium* sp. in SG (Table 3). Unfortunately, the low number of records did not allow the application of the model for the two additional *Kryptoperidinium* cell density classes, i.e., $>2 \times 10^5$ cells L^{-1} and $>3 \times 10^5$ cells L^{-1}. The GLMs for the entire data series showed that Sal, DIN and Rain significantly influenced the presence of *Kryptoperidinium* sp. in the two lagoons (Table 3). Moreover, DIN significantly influenced *Kryptoperidinium* sp. at the threshold of 2×10^5 cells L^{-1} and 3×10^5 cells L^{-1} (data not shown).

3.2 Morphological and phylogenetic analyses

Wild and cultured *Kryptoperidinium* cells from CA and SG lagoons shared the same morphology. They were oval in the ventral view (Fig. 6A) and strongly dorso-ventrally flattened, with concave ventral and convex dorsal sides, possessing a ‘comma’ shaped eyespot localized centrally within the hypotheca (Fig. 6A). The cells were 22.0–40.0 µm long (mean 30.7 ±3.7 µm, n=104), and 15.0–40.8 µm wide (mean 28.7 ±4.2 µm, n=104). No significant differences were detected in cell length between CA and SG strains or between CA and SG wild cells. Cell width showed no significant differences between CA and SG strains, however, the wild cells of SG were significantly wider than those from CA (mean widths of 32.6 ±4.7 µm and 28.5 ±3.2 µm for SG and CA, respectively). In both cultured strains and wild samples, chloroplasts were numerous and oval (Fig. 6A-B). Nuclear staining by DAPI revealed the presence of two nuclei. The bigger one, ellipsoidal in shape, was the dinokaryon and the smaller rounded to irregularly shaped one was the endosymbiotic nucleus

(Figure 6C). All cells examined were binucleate. The thecal plate pattern was Po, x, 4', 2a, 7", 5C, 5 – 6s, 5"', 2"" (Fig. 6D-I). Thecal plates were finely ornamented with small pores (Fig. 6J-K). The cingulum was ascending (Fig. 6D-F). Two plates showed a unique shape: the first apical plate (1') was wide and kidney-shaped with a more or less defined concavity in the left side formed by the anterior sulcal plate (sa) (Fig. 6D-F) and the 7" plate was very narrow and L-shaped, with a characteristic elongated and thin border inserted between the 1' plates and the 5C plate (Fig. 6D-G). The SSU, LSU rDNA and ITS molecular sequences obtained for both Sardinian strains were identical. The constructed phylogeny for SSU rDNA (Fig. 7) showed that the sequences were included within Kryptoperidiniaceae, which showed maximum support. This clade included all species belonging to *Unruhdinium* genus (maximum support, 100%/1), *Durinskia* (maximum support), *Galeidinium* (maximum support), and *Blixaea quinquecornis*. Sequences belonging to *Kryptoperidinium* clustered together, and split into two different clades, although statistical support was low (<85%/0.95), and they formed a sister clade with *Galeidinium* representatives (100%/1). Each *Kryptoperidinium* cluster showed maximum support. The first cluster included sequences from this study, other sequences obtained from the Mediterranean Sea, and a sequence belonging to representatives from the Baltic Sea. The second cluster included sequences from a strain obtained from Puerto Rico (Caribbean Sea). The topology with sequences available for the other rDNA regions was almost identical. In the case of LSU rDNA phylogeny (Supplementary Fig. 1), all *Kryptoperidinium* sequences were clustered together (100%/1), including sequences from this study, other Mediterranean areas, and one from the Atlantic Ocean (near Assateague Island, Maryland, USA). Two sequences obtained from the Caspian Sea formed a sub-cluster within this group (99%/1). In this case, sequences for the strain obtained in Puerto Rico were not available. In the case of the 5.8S rDNA phylogeny (Supplementary Fig. 2), *Kryptoperidinium* sequences were clustered into two different clades and showed a statistical support of 92%/1. Again, one cluster (100%/1) included sequences from this study and the Aegean Sea (Mediterranean), and the second (100%/1) included sequences from a strain from Puerto Rico. Finally, the concatenated tree (Fig. 8) showed the same topology for *Kryptoperidinium* sequences, with sequences from the Mediterranean Sea clustering together (100%/1), and those from Puerto Rico forming a sister cluster. The SSU rDNA sequence of the endosymbiont was only obtained for the KryCA_Uniss strain. It was identical (overlapping in 402 positions) to a *Kryptoperidinium* endosymbiont sequence available for an Aegean Sea strain in the Mediterranean. However, it showed 99.3% similarity (overlapping in 738 positions) with another available sequence of *Kryptoperidinium* endosymbiont from an unknown origin (data not shown).

373 3.4 Exponential growth rates in culture

374 Exponential growth rates for the SG strain varied from 0.17 day^{-1} to 0.33 day^{-1} at 11 °C and from
375 0.15 day^{-1} to 0.31 day^{-1} at 20 °C. Values were similar for CA, varying from 0.14 day^{-1} to 0.33 day^{-1}
376 at 11 °C and from 0.18 day^{-1} to 0.31 day^{-1} at 20 °C (Fig. 9). For both strains, no growth was
377 observed at 30 °C. The SG strain showed the highest exponential growth rate at a salinity of 30 at
378 both temperatures, whereas the CA strain showed the highest exponential growth rate at a salinity
379 of 40 at 11 °C and at a salinity of 10 at 20 °C (Fig. 9). No significant differences were detected
380 between the two temperatures in any of the salinity treatments, nor between the two strains or for
381 each strain. Exponential growth rates significantly differed between SG and CA strains in the 10
382 ($p < 0.01$) and 40 ($p < 0.05$) salinity treatments. The exponential growth rates of the SG strain also
383 differed significantly between the 30 salinity treatment and the 10 ($p<0.01$), 20 ($p<0.05$) and 40
384 ($p<0.05$) salinity treatments. The CA strain showed no significant differences among the salinity
385 treatments.
386
387 4. Discussion

388 The present study makes a valuable contribution to the ecology of a potentially harmful species of
389 the genus *Kryptoperidinium*, deepening some morphological and phylogenetic aspects. The
390 information obtained derives from field and from culture data, on two new isolates from different
391 lagoons in Sardinia. The reported data are among the few obtained for distinct and ecologically
392 important systems such as coastal shallow lagoons.
393
394 4.1 Morphology and taxonomy

395 The *Kryptoperidinium* cells from the CA and SG lagoons analyzed in this study shared the same
396 morphology and they were, therefore, from the same species. The phylogeny supported this
397 conclusion. The shape and size of *Kryptoperidinium* cells from the two lagoons conformed closely
398 to those previously reported by Biecheler (1952), Dodge (1982), Sournia (1986), Trigueros et al.
399 (2000), Kempton et al. (2002), Wolny et al. (2004) and Saburova et al. (2012). There is some
400 variability in the plate tabulation shown in the literature, especially in the number and shape of
401 epithecal and cingular plates (Biecheler, 1952; Dodge, 1982; Sournia, 1986; Trigueros et al., 2000;
402 Kempton et al., 2002; Wolny et al., 2004; Figueroa et al., 2009, Saburova et al., 2012 and
403 Gottschling et al., 2019). In this study, the plate formula of cells was determined as Po, X, 4′, 2a,
404 7″, 5C, 5 – 6s, 5‴, 2′′′′ which matched that reported by Kempton et al. (2002) and Gottschling et al.
405 (2019).

The peculiar kidney-shaped 1' plate observed in *Kryptoperidinium* sp. cells from CA and SG has been reported in Mediterranean and Atlantic cells (Biecheler, 1952; Trigueros et al., 2000; Kempton et al., 2002; Figueroa et al., 2009, and Gottschling et al., 2019), but more irregularly shaped 1' plates are also reported in the literature (Kempton et al., 2002; Wolny et al., 2004; Saburova et al., 2012). The narrow and L-shaped 7" plate seems to be a characteristic common to all the *Kryptoperidinium* described so far (Biecheler, 1952; Dodge, 1982; Sournia, 1986; Trigueros et al., 2000; Kempton et al., 2002; Wolny et al., 2004; Figueroa et al., 2009, Saburova et al., 2012 and Gottschling et al., 2019), whereas the theca finely ornamented by pores, as observed in this study, is only reported by Biecheler (1952). Almost all the aforementioned studies refer to the species *K. foliaceum*. However, Gottschling et al. (2018, 2019) recently highlighted difficulties with the nomenclature of *Kryptoperidinium* and, together with Kretschmann et al. (2018), provided evidence of at least two species within the genus. Consequently, pending further investigations, the species found in the studied lagoons is reported as *Kryptoperidinium* sp.

Cells from the two lagoon sites possessed the other two characteristics frequently reported in *Kryptoperidinium*: the presence of an endosymbiontic nucleus and of an eye spot. Both these features seemed to be peculiar to *Kryptoperidinium* although populations without the endosymbiont (Kempton et al., 2002; Gottschling et al., 2019) and the eye spot (Kempton et al., 2002; Saburova et al., 2012) have also been reported. In addition, degeneration of the eye spot in old cultures has been demonstrated (Moldrup et al., 2013).

The molecular data includes the strains obtained in this study in the Kryptoperidiniaceae, within a well-defined group that contains the available *Kryptoperidinium* sequences. The *Kryptoperidinium* cluster splits into two clades in all phylogenies, as reported in several studies (Gottschling and McLean, 2013, Kretschmann et al., 2018, Žerdoner Čalasan et al., 2018 and Gottschling et al., 2019). The first clade includes the strains obtained in this study together with strains from diverse localities (e.g., the Baltic, Mediterranean and North Atlantic) and the second includes a strain from Puerto Rico (UTEX1688). The second clade should also include other two strains (SC from the North Atlantic and NCMA 1326 from the North Pacific) as demonstrated by Kempton et al. (2002), Kretschmann et al. (2018), and Gottschling et al. (2019).

Reconstructing the morphological differences between the representatives of the two clades is particularly difficult due to the lack of information for the majority of strains, including that from the type locality (Baltic Sea) (Gottschling et al., 2019). Following the observations by Kempton et al. (2002), the cingulum orientation may be a criterion. The strains analyzed in this study and the Mediterranean strain GeoB 459 (Fig. 2; Gottschling et al., 2019) show an ascending cingulum, whereas Kempton et al. (2002) describe a descending cingulum for the strains attributed to the

second clade. The number of cingular plates is also proposed as a possible criterion (Gottschling et al., 2019) and the results of this study corroborate this proposal. The strains analyzed here possess five cingular plates as reported for some other strains of the first clade (Gottschling et al., 2019). Further data, including those from the type locality of *Kryptoperidinium foliaceum* (proposed to be renamed *K. triquetrum* by Gottschling et al., 2019), are needed to clarify the species-specific relationships among the *Kryptoperidinium* clades. However, the results obtained in this study contribute to create a useful knowledge base on the morphology and phylogeny of Mediterranean isolates. These data will be especially important for the future taxonomic evaluation of the *Kryptoperidinium* genus.

4.2 Ecology of *Kryptoperidinium* sp. from Mediterranean shallow coastal lagoons

Kryptoperidinium populations possess strong eurythermic and euryhaline characteristics and they have been reported in very diverse environmental conditions (Jenkinson, 1990; Johnston and Gilliland, 2000; Trigueros and Orive, 2000; Trigueros et al., 2000; Kempton et al., 2002; Wolny et al., 2004; Lopez-Flores et al., 2006; Lewitus et al., 2008; Figueroa et al., 2009; Saburova et al., 2012). Data obtained in this study confirm this ecological plasticity although the species showed a preference for the ecological conditions in CA. In CA, *Kryptoperidinium* gave rise to water discolorations. These events strongly influenced the ecosystem functions of the adjacent coastal areas, especially in summer and in relation to cultural ecosystem services. Local newspapers and media reported economic losses because of a decrease in tourists linked to the unpleasant sea conditions and increasing public alarm was signaled by tourist operators. Although shellfish and fish mortality events were reported during *Kryptoperidinium* blooms in South Carolina estuaries (Lewitus et al., 2003; Wolny et al., 2004) and in Tunisian coastal waters (Turki et al., 2007), this did not occur in CA.

CA is characterized by a rainier climate, lower salinity, and higher inorganic nutrient concentrations than SG. The two lagoons also differ in terms of size, shape, freshwater inputs, outlets, catchment area and human activities within the catchments (Pulina et al., 2017). In the present study, salinity and nutrients significantly differentiated the two lagoons as reported in previous studies at annual (Pulina et al., 2017; Pulina et al., 2018) and pluriannual scales (Bazzoni et al., 2013). In addition, the specific features of each lagoon were demonstrated to be fundamental drivers of the taxonomic composition and ecological traits of phytoplankton (Pulina et al., 2018). Therefore, lower salinity values and higher nutrient concentrations could be assumed to play a key role in the presence and especially in the intense blooms of *Kryptoperidinium* sp. in coastal Mediterranean lagoons.

Kryptoperidinium blooms have been associated with spring tidal variations and strong vertical and

474 horizontal salinity gradients, resulting in the retention of growing cells in the innermost areas of
475 North Atlantic estuaries where salinity levels are lower (Jenkinson, 1990; Orive et al., 1998;
476 Trigueros and Orive, 2000). However, summer blooms at high temperatures and salinities have
477 been recorded in Mediterranean lagoons (Lopez-Flores et al., 2006; Turki et al., 2007). The present
478 study shows both spring and summer blooms of *Kryptoperidinium* sp. in the same lagoon, which
479 suggests that the species is adaptable to a wide range of temperature and salinity at the same site.
480 Growth experiments showed a fair tolerance to different temperature and salinity conditions in both
481 the analyzed strains, similar to the field results. *Kryptoperidinium* sp. grew at both winter and
482 spring temperatures (11 °C and 20 °C), but no growth was observed at the highest temperature
483 tested (30 °C). Results did not indicate a significant difference between growth rates at 11 °C and
484 20 °C for either lagoon strain. Conversely, a preference for higher temperatures, with significantly
485 higher doubling rates at 19 °C and 23 °C compared to 15 °C have been observed for a
486 *Kryptoperidinium* strain from the Spanish Atlantic coast (reported as *K. foliaceum*, Figueroa et al.,
487 2009). The growth experiments also revealed comparable growth rates in all salinity treatments for
488 the strain from CA. Conversely, the strain from SG showed a preference for a salinity of 30 and
489 significantly lower growth rates in the 10 and 40 salinity treatments. These results underline a
490 difference in the response of the two strains to particular salinity conditions. These findings suggest
491 more adaptability in the CA strain, which comes from a more variable environment in terms of
492 salinity conditions at both spatial and temporal scales (Pulina et al., 2017).
493 The field and laboratory dataset obtained in this study suggests an indirect preference for lower
494 salinity in the field, probably connected to the rain-driven nutrient runoff from the catchment. The
495 GLMs revealed a significant correlation between *Kryptoperidinium* sp. and the DIN in both
496 lagoons. Interestingly, *Kryptoperidinium* growth, promoted by the artificial enrichment of inorganic
497 nitrogen in absence of silicate, was demonstrated in microcosm experiments in the Guadiana
498 estuary (southwestern Mediterranean Sea; Domingues et al., 2011). The influence of rain-driven
499 nutrient runoff was also described in South Carolina, with an association between blooms and the
500 input of organic compounds (Wolny et al., 2004).
501 Understanding the observed summer blooms that coincided with low nutrient levels in the absence
502 of rainfall is more complicated but intriguing. CA receives urban waste water treated by a sewage
503 treatment plant all year round and in summer this input increases, in relation to a doubling of the
504 human population because of tourists (especially Alghero, B.M. Padedda, person. comm.). The
505 inflow of waters enriched with organic nutrients could be the trigger for summer blooms in CA,
506 similarly to South Carolina (Wolny et al., 2004).

In summary, the ecological success of *Kryptoperidinium* sp. in the studied ecosystems is certainly linked to its wide environmental tolerance and plasticity. Its life history is important also in these ecosystems. The production of both sexual and asexual cysts with a very short dormancy period reinforces adaptability to highly variable environments (Figueroa et al., 2009). Cysts of the species were found in SG sediments at low densities (Satta et al., 2014), whereas CA sediments had very high densities of cysts (C.T. Satta, unpublished data). The species is able to grow in wide temperature and salinity ranges as demonstrated by field and laboratory data. However, the differences in the growth rates with different salinity treatments could suggest a slightly intraspecific variability that may explain the varying success of *Kryptoperidinium* sp. in the field. Intraspecific differences in ecophysiological responses and traits in strains of the same population and among different populations, even those that are genetically similar, have been demonstrated in numerous studies on other harmful dinoflagellates (e.g., *Alexandrium ostenfeldii*, Kremp et al., 2012; Van de Wall et al., 2015; Brandenburg et al., 2018). This variability is particularly important for populations faced with changing environmental conditions in the context of ongoing climate change (Kremp et al., 2012) and it could also be important in highly variable and disturbed environments such as Mediterranean lagoons. Results seem to suggest a role for nutrient (i.e., inorganic nitrogen) availability. However, the role of nutrients in promoting *Kryptoperidinium* growth must be considered with caution. Despite the established relationship between eutrophication and the increase of harmful algal blooms (Heisler et al., 2008), the response of *Kryptoperidinium* to nutrient availability may be affected by the possible mixotrophy of the species as already observed for other dinoflagellate species (Jeong et al., 2010 and references therein); by competition with other phytoplankton species (Litchman et al., 2012); and by consumer pressure (Boyce et al., 2015).

Further studies are needed to better understand the ecology of *Kryptoperidinium* species by investigating the role of both organic and inorganic nutrients, evidence for mixotrophy and the suspected intraspecific variability. This study underlines some interesting aspects of *Kryptoperidinium* dynamics that may be useful in subsequent ecological evaluations of the species.

Conclusions

The reconstruction of the *Kryptoperidinium* ecology through field and laboratory data allowed underlining the great plasticity of these dinoflagellates once again. The evidence gathered showed that blooms might arise at different environmental conditions also at the same site. Furthermore, highly variable environmental conditions promoted the presence and blooms of *Kryptoperidinium*.

Integrating multiannual ecological field data, laboratory experiments and the morphological and

molecular characterization of potentially harmful species are of particular importance in understanding their adverse effects in key ecosystems such as coastal Mediterranean lagoons. In addition, this base of knowledge inserted in a wide ecological framework can contribute to explain more complex ecological processes in aquatic ecosystems. In fact, the understanding of ecological processes and the integration of knowledge are particularly useful for designing common policies and sustainable management actions in aquatic ecosystems (Pérez-Ruzafa et al., 2011).

Acknowledgments

The authors thank Dott. Bastianina Manca and Dott. Pasqualina Farina for the nutrient analysis. CTS was funded by a grant of Sardinian Region within the project "Santa Giusta – Indagine nello Stagno di Santa Giusta inerente la parte trofica e di identificazione delle criticità che possono portare alle crisi distrofiche" (DGR n° 42/34 del 16/ 10/2013). The activities of Prof. Antonella Lugliè were supported by the research fund of the University of Sassari (Fondo di Ateneo per la Ricerca 2019).

References

Adachi, M., Sako, Y., Ishida, Y., 1994. Restriction fragment length polymorphism of Ribosomal DNA internal transcribed spacer and 5.8s- regions in Japanese *Alexandrium* Species (Dinophyceae). J. Phycol. 30, 857–863.

Bazzoni, A.M., Pulina, S., Padedda B.M., Satta C.T., Lugliè A., Sechi, N., Facca, C., 2013. Water quality evaluation in Mediterranean lagoons using the Multimetric Phytoplankton Index (MPI): Study cases from Sardinia. Transit. Waters Bull. 7(1), 64–76.

Biecheler, B., 1952. Recherche sur les peridinens. Bull. biol. Fr. Bel. 36, 1–149.

Boyce, D.G., Frank, K.T., Leggett, W.C., 2015. From mice to elephants: overturning the 'one size fits all' paradigm in marine plankton food chains. Ecol. Lett. 18, 504–515.

Brandenburg, K.M., Wohlrab, S., John, U., Kremp, A., Jerney, J., Krock, B., Van de Waal, D.B., 2018. Intraspecific trait variation and trade-offs within and across populations of a toxic dinoflagellate. Ecol. Lett. 21, 1561–1571.

Castresana, J., 2000. Selection of conserved blocks from multiple alignments for their use in phylogenetic analysis. Mol. Biol. Evol. 17, 540–52.

Dodge, J.D., 1971. A dinoflagellate with both a mesocaryotic and a eucaryotic nucleus. I. Fine structure of the nuclei. Protoplasma 73, 145–157.

Dodge, J.D., 1982. Marine dinoflagellates of the British Isles, Her Majesty's Stationery Office, London.

576 Dodge, J.D., Crawford, R.M., 1969. Observations on the fine structure of the eyespot and associated
577 organelles in the dinoflagellate *Glenodinium foliaceum*. J. Cell Sci. 5, 479–493.
578 Domingues, R.B., Anselmo, T.P., Barbosa, A.B., Sommer, U., Galvão, H.M., 2011. Nutrient
579 limitation of phytoplankton growth in the freshwater tidal zone of a turbid, Mediterranean estuary.
580 Estuar. Coast. Mar. Sci. 91, 282–297.
581 Ehrenberg, C.G., 1840. Blätter von ihm selbst ausgeführter Zeichnungen von eben sovielen Arten.
582 Bericht. Kgl. Preuss. Akad. Wiss. Berlin, 197–219.
583 Figueroa, R. I., Bravo, I., Fraga, S., Garces, E., Llaveria, G., 2009. The life history and cell cycle of
584 *Kryptoperidinium foliaceum*, a dinoflagellate with two eukaryotic nuclei. Protist 160, 285–300.
585 Fritz, L., Triemer, R.E., 1985. A rapid simple technique utilizing Calcofluor White M2R for the
586 visualization of dinoflagellate thecal plates. J. Phycol. 21, 662–664.
587 Gottschling, M., McLean, T.I., 2013. New home for tiny symbionts: Dinophytes determined as
588 *Zooxanthella* are Peridiniales and distantly related to *Symbiodinium*. Mol. Phylogenetics Evol. 67,
589 217–222.
590 Gottschling, M., Tillmann, U., Kusber, W.H., Hoppenrath, M., Elbrächter, M., 2018. A Gordian
591 knot: Nomenclature and taxonomy of *Heterocapsa triquetra* (Peridiniales: Heterocapsaceae). Taxon
592 67, 179–185.
593 Gottschling, M., Tillmann, U., Elbrächter, M., Kusber, W.H., Hoppenrath, M., 2019. *Glenodinium*
594 *triquetrum* Ehrenb. is a species not of *Heterocapsa* F.Stein but of *Kryptoperidinium* Er.Lindem.
595 (Kryptoperidiniaceae, Peridiniales). Phytotaxa,391(2), 155–158.
596 Guillard, R.R.L., 1973. Division rates. In: Stein, J. R. (Ed.), Handbook of Phycological Methods:
597 Culture Methods and Growth Measurements. Cambridge University Press, Cambridge, pp. 289–
598 311.
599 Guillard, R.R.L., Hargraves, P.E., 1993. *Stichochrysis immobilis* is a diatom, not a chrysophyte.
600 Phycologia 32(3), 234–236.
601 Heisler, J., Glibert, P.M., Burkholder, J.M., Anderson. D.M., Cochlan, W., Dennison, W.C.,
602 Dortch, Q., Gobler, C.J., Heil, C.A., Humphries, E., Lewitus, A., Magnien, R., 2008. Eutrophication
603 and harmful algal blooms: A scientific consensus. Harmful Algae 8, 3–13.
604 Janouškovec, J., Gavelis, G.S., Burki, F., Dinh, D., Bachvaroff, T.R., Gornik, S.G., Bright, K.J.,
605 Imanian, B., Strom, S.L., Delwiche, C.F., Waller, R.F., Fensome, R.A., Leander, B.S., Rohwer,
606 F.L., Saldarriaga, J.F., 2017. Major transitions in dinoflagellate evolution unveiled by
607 phylotranscriptomics. Proc. Natl. Acad. Sci. USA 114(2), E171–E180.

Jenkinson, I. R., 1990. Estuarine plankton of Co Limerick. I. A recurrent summer bloom of *Glenodinium foliaceum* Stein confined to the Deel estuary, with data on micro- plankton biomass. Ir. Nat. J. 23(5/6), 173□–180.

Jeong, H.J., Yoo, Y.D., Kim, J.S., Seong, K.A., Kang, N.S., Kim, T.H., 2010. Growth, Feeding and Ecological Roles of the Mixotrophic and Heterotrophic Dinoflagellates in Marine Planktonic Food Webs. Ocean Sci. J. 45(2), 65–91.

Johnston, C.M., Gilliland, P.M., 2000. Investigating and managing water quality in saline lagoons based on a case study of nutrients in the Chesil and the Fleet European marine site. English Nature (UK Marine SACs Project), 141 pp.

Katoh, K., Misawa, K., Kuma, K., Miyata, T., 2002. MAFFT: a novel method for rapid multiple sequence alignment based on fast Fourier transform. Nucleic Acids Res. 30, 3059–3066.

Kempton, J.W., Wolny, J., Tengs, T., Rizzo, P., Morris, R., Tunnell, J., Scott, P., Steidinger, K., Hymel, S.N., Lewitus, A.J., 2002. *Kryptoperidinium foliaceum* blooms in South Carolina: a multianalytical approach to identification. Harmful Algae 1, 383–392.

Kremp, A., Godhe, A., Egardt, J., Dupont, S., Suikkanen, S., Casabianca, S., Penna, A., 2012. Intraspecific variability in the response of bloom-forming marine microalgae to changed climate conditions. Ecol. Evol. 2(6), 1195–1207.

Kretschmann, J., Žerdoner Čalasan, A., Gottschling, M., 2018. Molecular phylogenetics of dinophytes harbouring diatoms as endosymbionts (Kryptoperidiniaceae, Peridiniales), with evolutionary interpretations and a focus on the identity of *Durinskia oculata* from Prague. Mol. Phylogenetics Evol. 118, 392–402.

Lebour, M.V., 1925. The dinoflagellates of northern seas. Marine Biological Association of the United Kingdom, Plymouth.

Lewitus, A.J., Schmidt, L.B., Mason, L.J., Kempton, J.W., Wilde, S.B., Wolny, J.L., Williams, B.J., Hayes, K.C., Hymel, S.N., Keppler, C.J., Ringwood, A.H., 2003. Harmful algal blooms in South Carolina residential and golf course ponds. Popul. Environ. 24, 387–413.

Lewitus, A.J., Brock, L.M., Burke, M.K., DeMattio, K.A., Wilde, S.B., 2008. Lagoonal stormwater detention ponds as promoters of harmful algal blooms and eutrophication along the South Carolina coast. Harmful Algae 8, 60–65.

Lin, S., Zhang, H., Hou, Y., Miranda, L., Bhattacharya, D., 2006. Development of a dinoflagellate-oriented PCR primer set leads to detection of picoplanktonic dinoflagellates from Long Island Sound. Appl. Environ. Microbiol. 72, 5626 –5630.

Lindemann, V.E., 1924. Der *Kryptoperidinium foliaceum* (Stein) n. nom. (Zugleich eine vorlaüfige Mitteilung). Archiv für Botanisches 5, 114–120.

642 Litchman, E., Edwards, K.F., Klausmeier, C.A., Thomas, M.K., 2012. Phytoplankton niches, traits
643 and eco-evolutionary responses to global environmental change. Mar. Ecol. Prog. Ser. 470, 235–
644 248.
645 Logares, R., Shalchian-Tabrizi, K., Boltovskoy, A., Rengefors, K., 2007. Extensive dinoflagellate
646 phylogenies indicate infrequent marine–freshwater transitions. Mol. Phylogenetics Evol. 45, 887–
647 903.
648 Lopez-Flores, R., Garcés, E., Boix, D., Badosa, A., Brucet, S., Maso, M., Quintana, X.D., 2006.
649 Comparative composition and dynamics of harmful dinoflagellates in Mediterranean salt marshes
650 and nearby external marine waters. Harmful Algae 5, 637–648.
651 McCullagh, P., Nelder, J.A., 1989. Generalized Linear Models. Chapman and Hall, London.
652 Medlin, L., Elwood, H.J., Stickel, S., Sogin, M.L., 1988. The characterization of enzymatically
653 amplified eukaryotic 16S- like rRNA- coding regions. Gene 71, 491–499.
654 Moldrup, M., Moestrup, Ø., Hansen, P.J., 2013. Loss of phototaxis and degeneration of an eyespot
655 in long-term algal cultures: Evidence from ultrastructure and behaviour in the dinoflagellate
656 *Kryptoperidinium foliaceum*. J. Eukaryot. Microbiol. 60, 327–334.
657 Newton, A., Icely, J., Cristina, S., Brito, A., Cardoso, A.C., Colijn, F., Dalla Riva, S., Gertz, F.,
658 Hansen, J.W., Holmer, M., Ivanova, K., Leppäkoski, E., Melaku Canu, D., Mocenni, C., Mudge, S.,
659 Murray, N., Pejrup, M., Razinkovas, A., Reizopoulou, S., Pérez-Ruzafa, A., Schernewski, G.,
660 Schubert, H., Carr, L., Solidoro, C., Viaroli, P., Zaldívar, J.M., 2014. An overview of ecological
661 status, vulnerability and future perspectives of European large shallow, semi-enclosed coastal
662 systems, lagoons and transitional waters. Estuar. Coast. Shelf Sci. 140, 95–122.
663 Newton, A., Brito, A.C., Icely, J.D., Derolez, V., Clara, I., Angus, S., Schernewski, G., Inácio, M.,
664 Lillebø, A.I., Sousa, A.I., Béjaoui, B., Solidoro, C., Tosic, M., Cañedo-Argüelles, M., Yamamuro,
665 M., Reizopoulou, S., Tseng, H.-C., Canu, D., Roselli, L., Maanan, M., Cristina, S., Ruiz-Fernández,
666 A.C., de Lima, R.F., Kjerfve, B., Rubio-Cisneros, N., Pérez-Ruzafa, A., Marcos, C., Pastres, R.,
667 Pranovi, F., Snoussi, M., Turpie, J., Tuchkovenko, Y., Dyack, B., Brookes, J., Povilanskas, R.,
668 Khokhlov, V., 2018. Assessing, quantifying and valuing the ecosystem services of coastal lagoons.
669 J. Nat. Conserv. 44, 50–65.
670 Orive, E., Iriarte, A., de Madariaga, I., Revilla, M., 1998. Phytoplankton blooms in the Urdaibai
671 estuary during summer: physico-chemical conditions and taxa involved. Oceanol. Acta 21, 293–
672 305.
673 Padedda, B.M., Pulina, S., Satta, C.T., Lugliè, A., Magni, P., 2019. Eutrophication and Nutrient
674 Fluxes in Mediterranean Coastal Lagoons. In: Maurice, P. (Ed.), Encyclopedia of Water. John
675 Wiley and Sons, Inc., Hoboken, New Jersey (USA).

676 Paulsen, O., 1908. Peridiniales. In: Brandt, K., Apstein, C. (Eds.), Nordisches plankton. Botanischer
677 Teil, XVIII. Verlag von Lipsius und Tischer, Kiel, pp. 1–124.
678 Pérez-Ruzafa, A., Marcos, C., Pérez-Ruzafa, I.M., 2011. Mediterranean coastal lagoons in an
679 ecosystem and aquatic resource management context. Phys. Chem. Earth. 36, 160–166.
680 Pienaar, R.N., Sakai, H., Horiguchi, T., 2007. Description of a new dinoflagellate with a diatom
681 endosymbiont, *Durinskia capensis* sp. nov. (Peridiniales, Dinophyceae) from South Africa. J. Plant
682 Res. 120, 247–258.
683 Prager, J.C., 1963. Fusion of the family Glenodiniaceae into the Peridiniaceae, with notes on
684 *Glenodinium foliaceum* Stein. J. Protozool. 10, 195–204.
685 Price, D. C., Bhattacharya, D., 2017. Robust Dinoflagellata phylogeny inferred from public
686 transcriptome databases. J. Phycol. 53, 725–729.
687 Pulina, S., Satta, C.T., Padedda, B.M., Bazzoni, A.M., Sechi, N., Lugliè A., 2017.
688 Picophytoplankton Seasonal Dynamics and Interactions with Environmental Variables in Three
689 Mediterranean Coastal Lagoons. Estuar. Coast. 40, 469–478.
690 Pulina, S., Satta, C.T., Padedda, B.M., Sechi, N., Lugliè, A., 2018. Seasonal variations of
691 phytoplankton size structure in relation to environmental variables in three Mediterranean shallow
692 coastal lagoons. Estuar. Coast. Shelf Sci. 212, 95–104.
693 Ronquist, F., Teslenko, M., Van Der Mark, P., Ayres, D.L., Darling, A., Höhna, S., Larget, B., Liu,
694 L., Suchard, M.A., Huelsenbeck, J.P., 2012. MrBayes 3.2: efficient Bayesian phylogenetic
695 inference and model choice across a large model space. Syst. Biol. 61, 539–542.
696 Saburova, M., Polikarpov, I., Al-Yamani, F., 2012. First record of *Kryptoperidinium foliaceum*
697 (Dinophyceae: Peridiniales) from a hypersaline environment in Kuwait, north-western Arabian
698 Gulf. Mar. Biodivers. Rec. 5, e104.
699 Satta, C.T., Anglès, S., Garcés, E., Sechi, N., Pulina, S., Padedda, B.M., Stacca, D., Lugliè, A.,
700 2014. Dinoflagellate cyst assemblages in surface sediments from three shallow Mediterranean
701 Lagoons (Sardinia, North Western Mediterranean Sea). Estuar. Coast. 37, 646–663.
702 Satta, C.T., Padedda, B.M., Sechi, N., Pulina, S., Loria, A., Lugliè, A., 2017. Multiannual
703 *Chattonella subsalsa* Biecheler (Raphidophyceae) blooms in a Mediterranean lagoon (Santa Giusta
704 Lagoon, Sardinia Island, Italy). Harmful Algae, 67, 61–73.
705 Schiller, J., 1937. In: Rabenhorst's Kryptogamen-Flora von Deutschland, Dr. L. (Ed.),
706 Dinoflagellatae (Peridineae) in monographischer Behandlung. Österreich und der Schweiz. Bd., pp.
707 321–480 10 (3) Teil 2 (3).

Scholin, C.A., Herzog, M., Sogin, M., Anderson, D.M. 1994. Identification of group- and strain-specific genetic markers for globally distributed *Alexandrium* (Dinophyceae). 2. Sequence analysis of a fragment of the LSU rRNA gene. J. Phycol. 30, 999–1011.

Sechi, N., Fiocca, F., Sannio, A., Lugliè A., 2001. Santa Giusta Lagoon (Sardinia): phytoplankton and nutrients before and after waste water diversion. J. Limnol. 60(2), 194–200.

Sournia, A., 1986. Atlas du Phytoplancton Marin, vol. 1. Introduction, Cyanophycees, Dictyochophycees, Dinophycees, et Raphidophycees. Centre National de la Recherche Scientifique, Paris, pp. 1–219.

Stamatakis, A., 2014. RAxML version 8: a tool for phylogenetic analysis and post-analysis of large phylogenies. Bioinformatics 30, 1312–1313.

Strickland, J.D.H., Parsons, T.R., 1972. A Practical Handbook of Seawater Analysis. Fisheries Research Board of Canada, Ottawa, Canada, pp. 167.

Takano, Y., Hansen, G., Fujita, D., Horiguchi, T., 2008. Serial replacement of diatom endosymbionts in two freshwater dinoflagellates, *Peridiniopsis* spp. (Peridiniales, Dinophyceae). Phycologia 47, 41–53.

Trigueros, J.M., Orive, E., 2000. Tidally driven distribution of phytoplankton blooms in a shallow, macrotidal estuary. J. Plankton Res. 22, 969 –986.

Trigueros, J.M., Ansotegui, A., Orive, E., 2000. Remarks on Morphology and Ecology of Recurrent Dinoflagellate Species in the Estuary of Urdaibai (Northern Spain). Bot. Mar. 43, 93–103.

Turki, S., Balti, N., Ben Salah, C., 2007. First detection of *Kryptoperidinium foliaceum* (Stein 1883) in Tunisian waters. Harmful Algae News 35, 9–10.

Utermöhl, H., 1958. Zurvervollkommung der quantitativenphytolankton-methodik. Mitt. d. Internat. Vereinig. f. Limnologie 9, 1–39.

Van de Waal, D.B., Tillmann, U., Martens, H., Krock, B., Van Scheppingen, Y., John, U., 2015. Characterization of multiple isolates from an *Alexandrium ostenfeldii* bloom in the Netherlands. Harmful Algae 49, 94–104.

Wolny, J.L., Kempton, J.W., Lewitus, A.J., 2004. Taxonomic Re-evaluation of a South Carolina ‘‘Red Tide’’ Dinoflagellate Indicates Placement in the Genus *Kryptoperidinium*. In: Steidinger, K.A., Landsberg, J.H., Tomas, C.R., Vargo, G.A. (Eds.), Harmful Algae 2002. Florida Fish and Wildlife Conservation Commission. Florida Institute of Oceanography and Inter-governmental Oceanographic Commission of UNESCO, St. Petersburg, Florida, pp. 443–445.

Zhang, H., Lin, S., 2005. Phylogeny of dinoflagellates based on mitochondrial cytochrome b and nuclear small subunit rDNA sequence comparisons. J. Phycol. 41, 411–420.

Zhang, Q., Guoxiang L., Hu, Z., 2011. Morphological differences and molecular phylogeny of freshwater blooming species, *Peridiniopsis* spp. (Dinophyceae) from China. Eur. J. Protistol. 47, 149–160.

Žerdoner Čalasan, A., Kretschmann, J., Gottschling, M., 2018. Absence of co-phylogeny indicates repeated diatom capture in dinophytes hosting a tertiary endosymbiont. Org. Divers. Evol. 18, 29–38.

Figure Captions

Figure 1 Location of Calich and Santa Giusta lagoons and sampling stations placement (black-filled circles) in Calich (1CA, 2CA and 3CA) and Santa Giusta (1SG, 2SG, 3SG and 4SG). Black arrows = freshwater inputs; white arrows = sea inlets.

Figure 2 Boxplots showing the monthly mean variability of rainfall (Rain), water temperature (Temp) and salinity (Sal), in Santa Giusta (SG) and Calich (CA) lagoons. Lines represent medians; M represent means. Bottom of box is the first quartile (Q1); upper part is the third quartile (Q3). Whiskers represent the 90th and 10th percentiles.

Figure 3 Boxplots showing the monthly mean variability of dissolved inorganic nitrogen (DIN), reactive phosphorous (PO4), and the ratio between DIN and PO4 (DIN:PO4), in Santa Giusta (SG) and Calich (CA) lagoons. Lines represent medians; M represent means. Bottom of box is the first quartile (Q1); upper part is the third quartile (Q3). Whiskers represent the 90th and 10th percentiles.

Figure 4 Monthly means of *Kryptoperidinium* cell density, rainfall (Rain), water temperature (Temp) and salinity (Sal) in Santa Giusta (SG) and Calich (CA) lagoons. Monthly means for Rain derived from the monthly accumulations (obtained summing daily rainfall values) averaged over the years (from 2011 to 2016 for SG and from 2008 to 2015 for CA). Monthly means for Temp and Sal derived from data obtained biweekly or monthly from May 2011 to September 2016 for SG and from September 2008 to June 2015 for CA. Vertical bars represent standard deviations of the mean.

Figure 5 Monthly means of *Kryptoperidinium* cell density, dissolved inorganic nitrogen (DIN), inorganic phosphorous (PO_4) and the ratio between DIN and PO_4 (DIN:PO_4), in Santa Giusta (SG)

and Calich (CA) lagoons. Monthly means for nutrients derived from data obtained biweekly or monthly from May 2011 to September 2016 for SG and from September 2008 to June 2015 for CA. Vertical bars represent standard deviations of the mean.

Figure 6 Morphology of *Kryptoperidinium* cells in light and epifluorescence microscopy from the Western Mediterranean Sea: ventral view of a living cell (A), shape of chloroplasts (B), position of the two nuclei, the dinokarion (dk) and the endosymbiontic nucleus (en) (C), plate pattern arrangement in ventral views (D-F), Po and x plate arrangement (G), plate pattern arrangement in dorsal views (H-I), and theca ornamentation (J-K). Scale bars represent 10 µm.

Figure 7 Maximum likelihood phylogenetic tree inferred from the SSU rDNA sequences of the family Kryptoperidiniaceae. The sequences of other peridinioid representatives are used as outgroup. Sequences obtained in this study are indicated in bold. The bootstrap values (BP) and the Bayesian posterior probabilities (BPP) are provided at each node (% BS/BPP). Only BS and BPP values >80% and >0.95, are shown.

Figure 8 Maximum likelihood phylogenetic tree inferred from the concatenated SSU, 5.8S and LSU rDNA sequences of the family Kryptoperidiniaceae. The sequences of other peridinioid representatives are used as outgroup. Sequences obtained in this study are indicated in bold. The bootstrap values (BP) and the Bayesian posterior probabilities (BPP) are provided at each node (% BS/BPP). Only BS and BPP values >80% and >0.95, are shown.

Figure 9 Exponential growth rates of *Kryptoperidinium* strains from SG and CA lagoons in the five salinity treatments, at 11 °C and 20 °C. Data points are an average of a minimum of 3 time points per treatment and vertical bars are standard deviations of the mean. No growth was observed at 30 °C for both strains.

Supplementary figure captions

Supplementary Figure 1 Maximum likelihood phylogenetic tree inferred from the LSU rDNA sequences of the family Kryptoperidiniaceae. The sequences of other peridinioid representatives are used as outgroup. Sequences obtained in this study are indicated in bold. The bootstrap values (BP) and the Bayesian posterior probabilities (BPP) are provided at each node (% BS/BPP). Only BS and BPP values >80% and >0.95, are shown.

Supplementary Figure 2 Maximum likelihood phylogenetic tree inferred from the 5.8S rDNA sequences of the family Kryptoperidiniaceae. The sequences of other peridinioid representatives are used as outgroup. Sequences obtained in this study are indicated in bold. The bootstrap values (BP) and the Bayesian posterior probabilities (BPP) are provided at each node (% BS/BPP). Only BS and BPP values >80% and >0.95, are shown.

Figure 1

Click here to access/download;Figure;Figure 1.tif

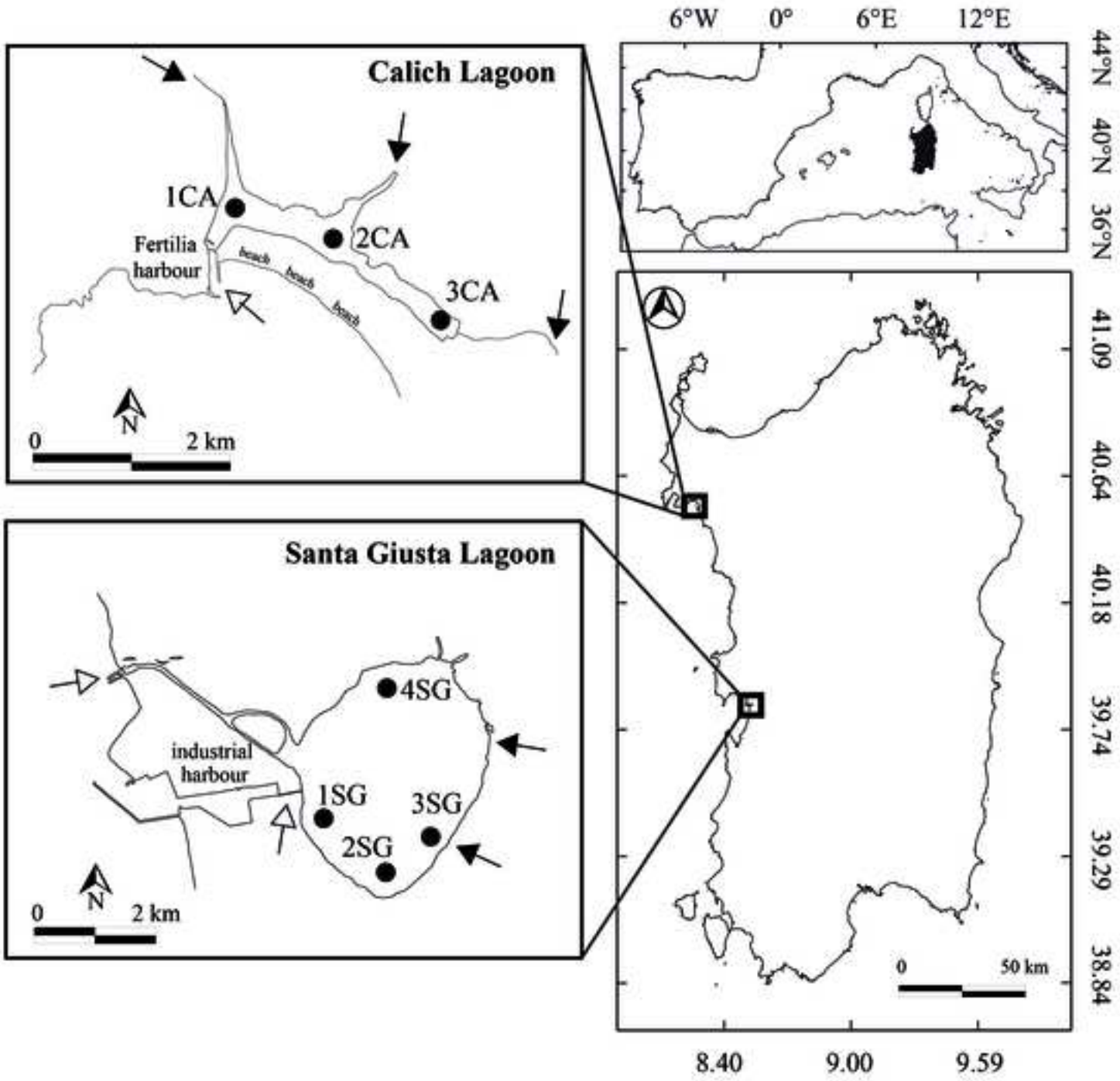

Figure 2

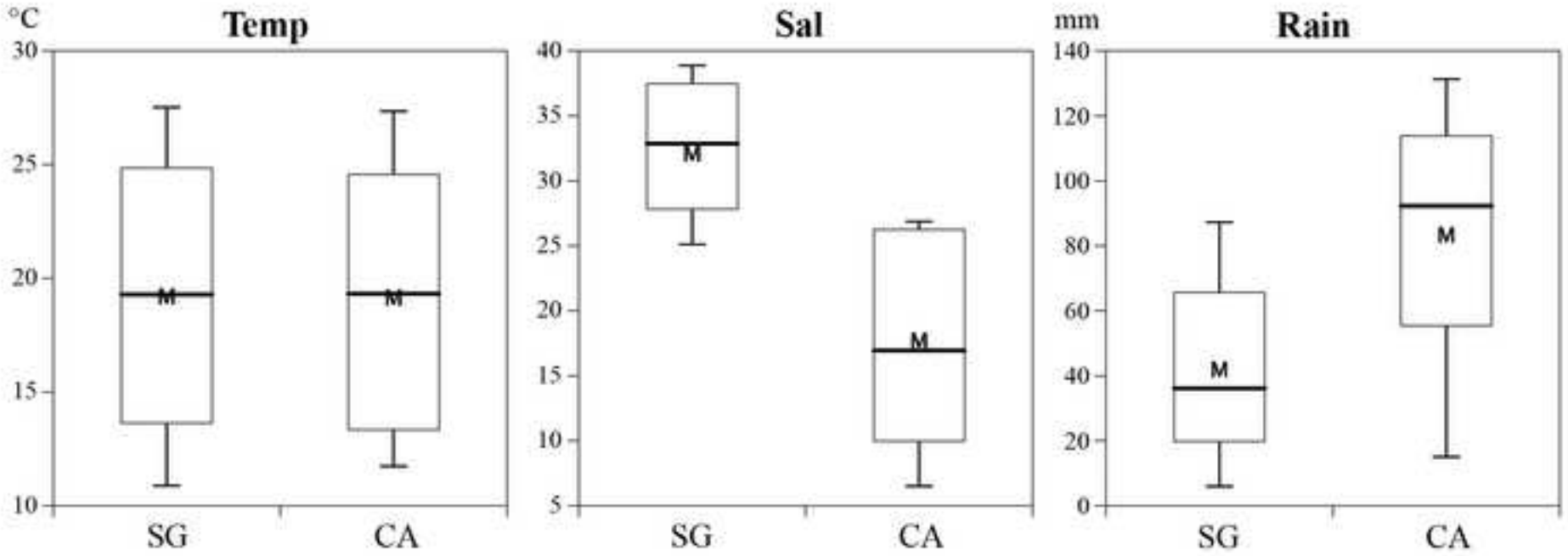

Figure 3

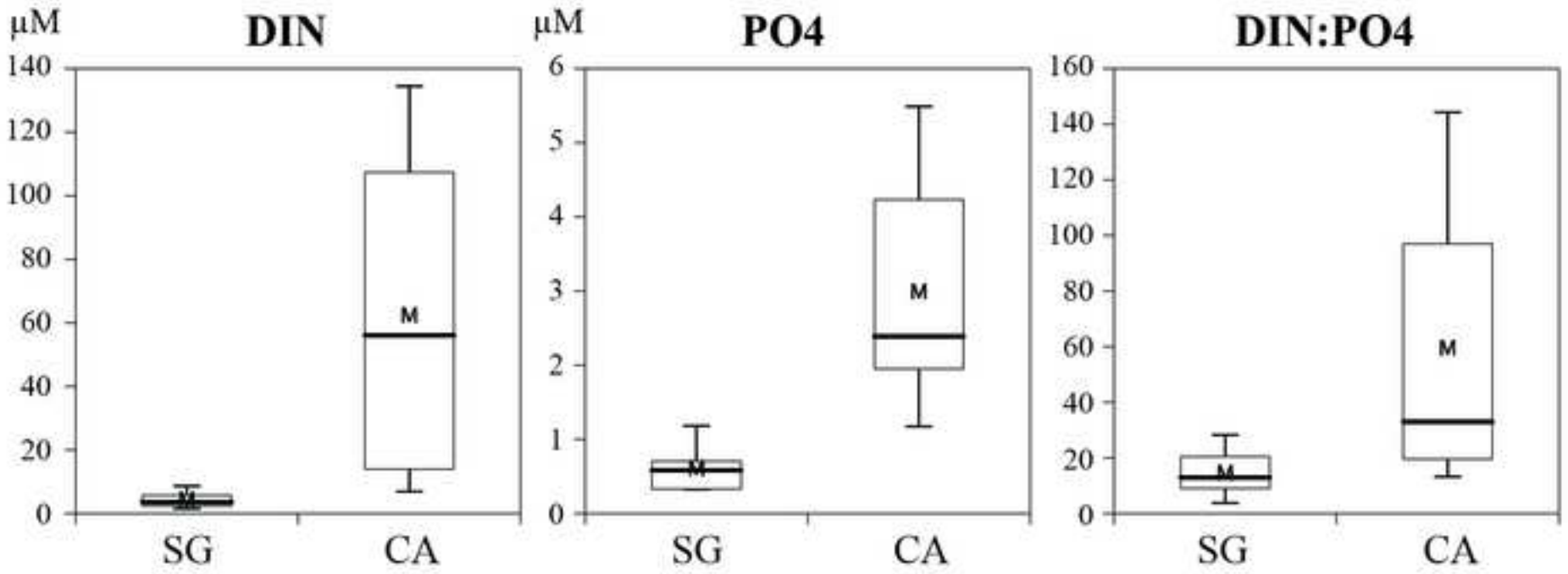

Figure 4

Click here to access/download;Figure;Figure 4.tif

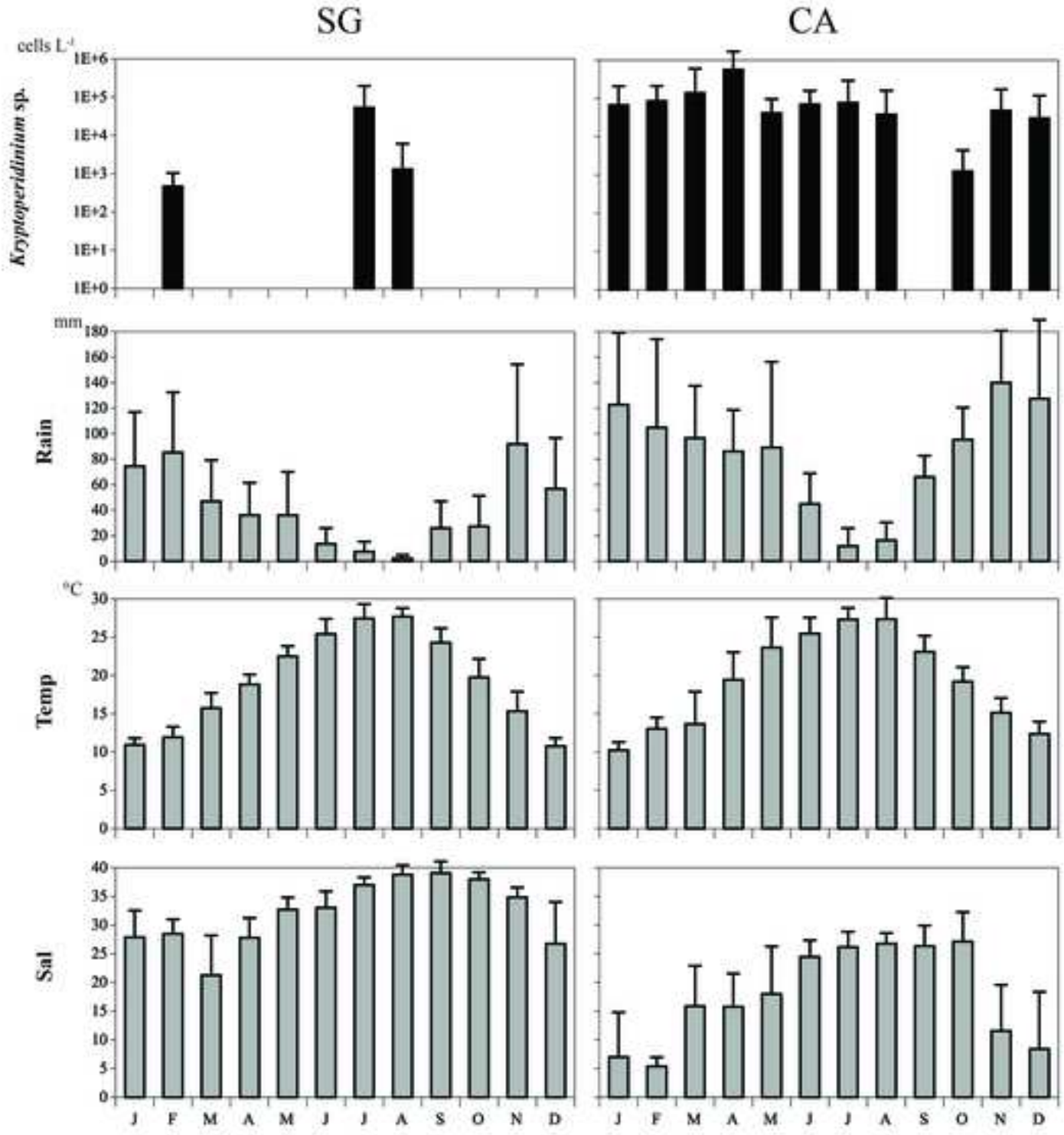

Figure 5

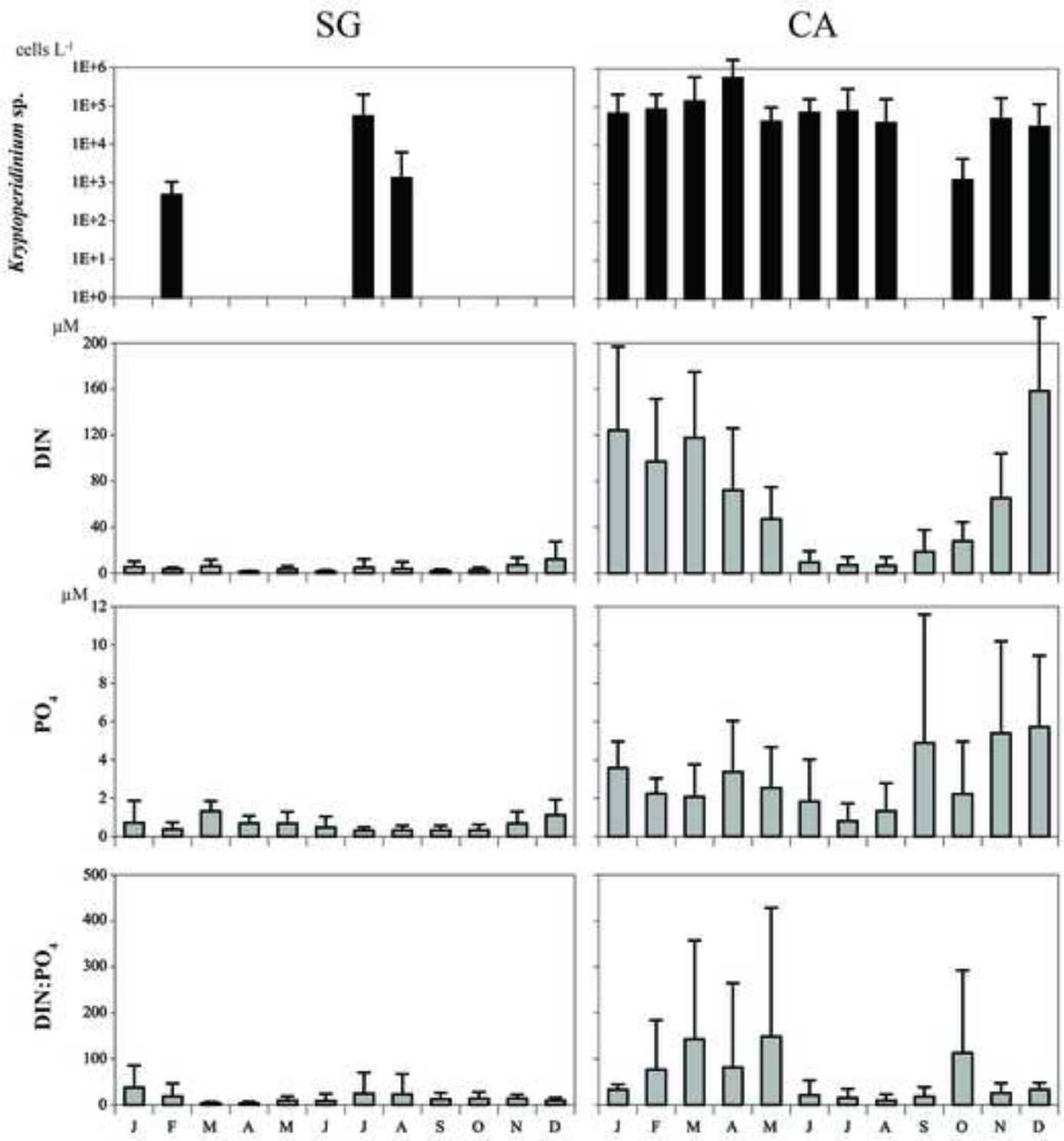

Figure 6

Click here to access/download;Figure;Figure 6.tif

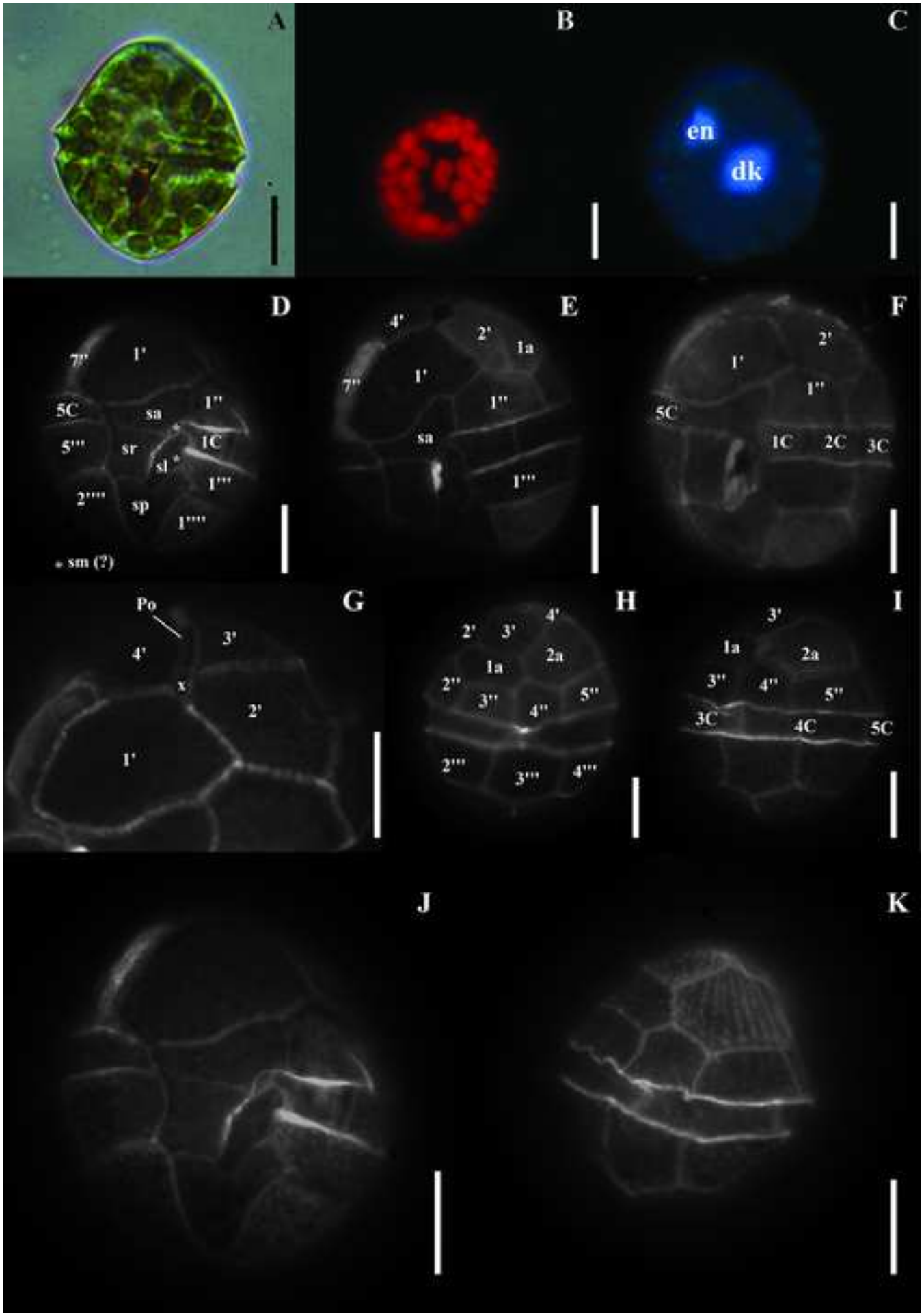

Figure 7

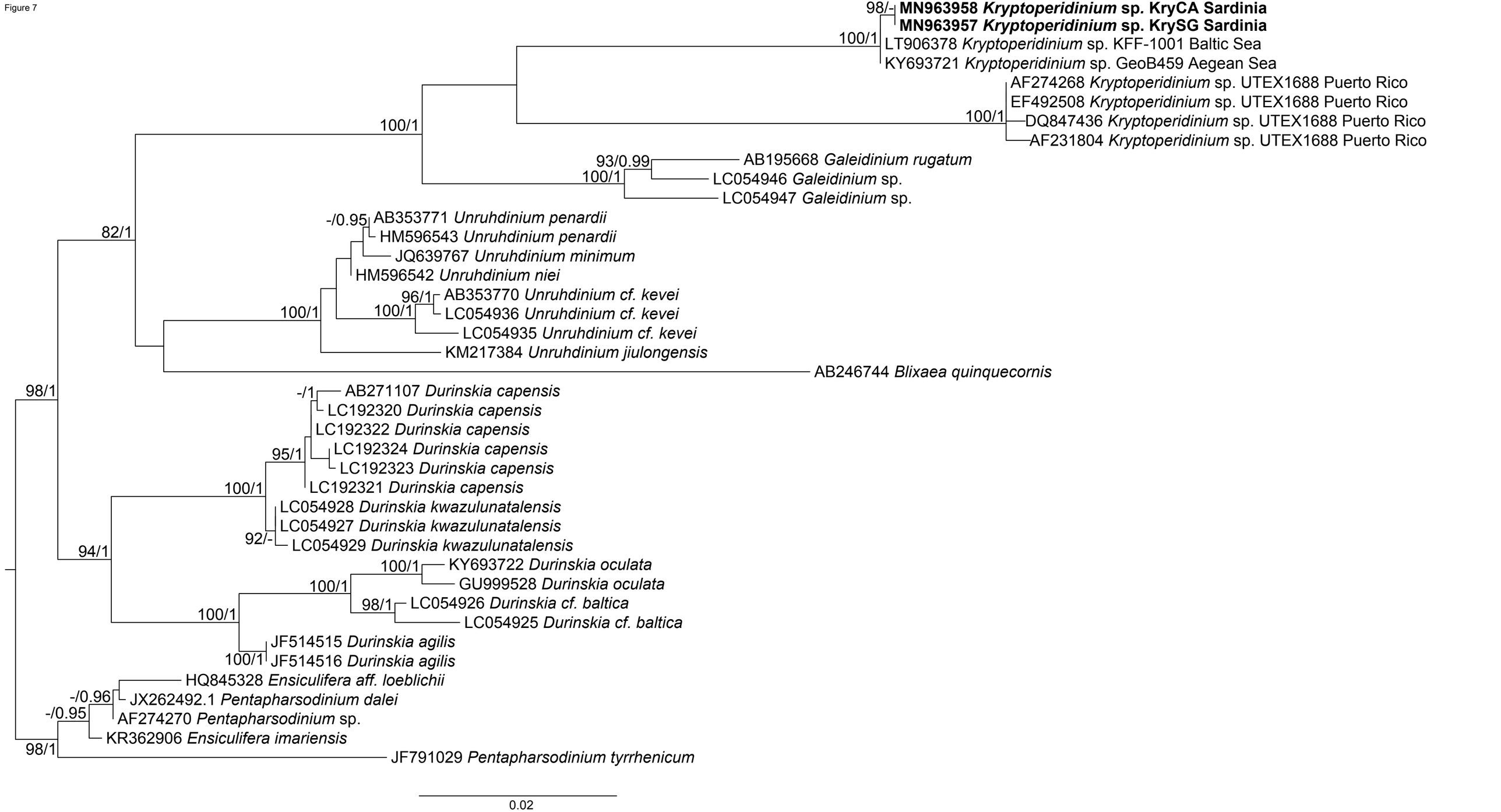
98/-
MN963958 Kryptoperidinium sp. KryCA Sardinia
MN963957 Kryptoperidinium sp. KrySG Sardinia
100/1
LT906378 Kryptoperidinium sp. KFF-1001 Baltic Sea
KY693721 Kryptoperidinium sp. GeoB459 Aegean Sea
AF274268 Kryptoperidinium sp. UTEX1688 Puerto Rico
EF492508 Kryptoperidinium sp. UTEX1688 Puerto Rico
100/1
DQ847436 Kryptoperidinium sp. UTEX1688 Puerto Rico
AF231804 Kryptoperidinium sp. UTEX1688 Puerto Rico
100/1
93/0.99
AB195668 Galeidinium rugatum
100/1
LC054946 Galeidinium sp.
LC054947 Galeidinium sp.
-/0.95
AB353771 Unruhdinium penardii
82/1
HM596543 Unruhdinium penardii
JQ639767 Unruhdinium minimum
HM596542 Unruhdinium niei
96/1
AB353770 Unruhdinium cf. kevei
100/1
100/1
LC054936 Unruhdinium cf. kevei
LC054935 Unruhdinium cf. kevei
KM217384 Unruhdinium jiulongensis
AB246744 Blixaea quinquecornis
98/1
-/1
AB271107 Durinskia capensis
LC192320 Durinskia capensis
LC192322 Durinskia capensis
95/1
LC192324 Durinskia capensis
LC192323 Durinskia capensis
100/1
LC192321 Durinskia capensis
LC054928 Durinskia kwazulunatalensis
LC054927 Durinskia kwazulunatalensis
92/-
LC054929 Durinskia kwazulunatalensis
94/1
100/1
KY693722 Durinskia oculata
100/1
GU999528 Durinskia oculata
98/1
LC054926 Durinskia cf. baltica
100/1
LC054925 Durinskia cf. baltica
JF514515 Durinskia agilis
100/1
JF514516 Durinskia agilis
HQ845328 Ensiculifera aff. loeblichii
-/0.96
JX262492.1 Pentapharsodinium dalei
-/0.95
AF274270 Pentapharsodinium sp.
KR362906 Ensiculifera imariensis
98/1
JF791029 Pentapharsodinium tyrrhenicum
0.02

Figure 8

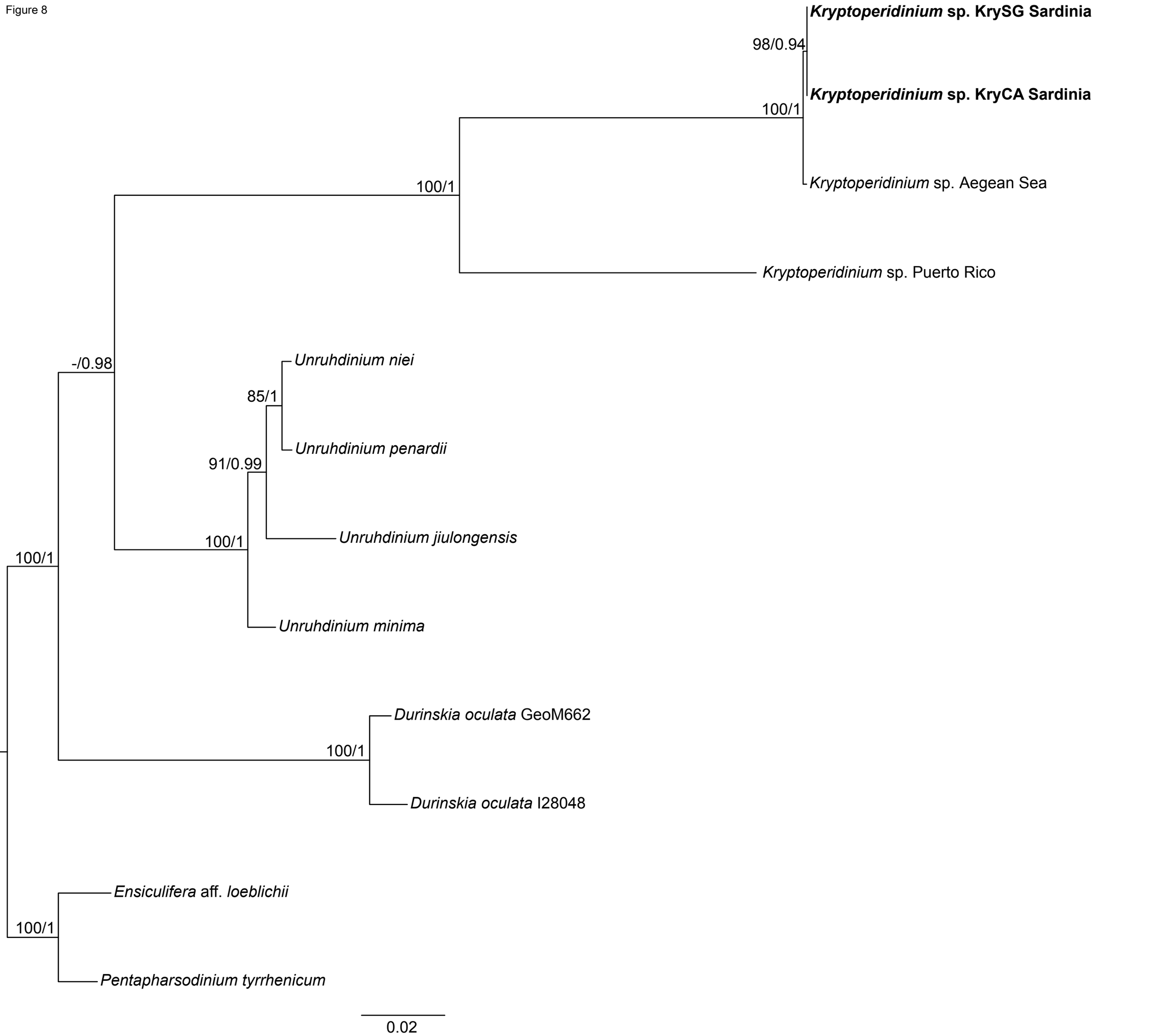
***Kryptoperidinium* sp. KrySG Sardinia**
98/0.94
***Kryptoperidinium* sp. KryCA Sardinia**
100/1
Kryptoperidinium sp. Aegean Sea
100/1
Kryptoperidinium sp. Puerto Rico
-/0.98
Unruhdinium niei
85/1
Unruhdinium penardii
91/0.99
Unruhdinium jiulongensis
100/1
Unruhdinium minima
100/1
Durinskia oculata GeoM662
100/1
Durinskia oculata I28048
Ensiculifera aff. *loeblichii*
100/1
Pentapharsodinium tyrrhenicum
0.02

Figure 9

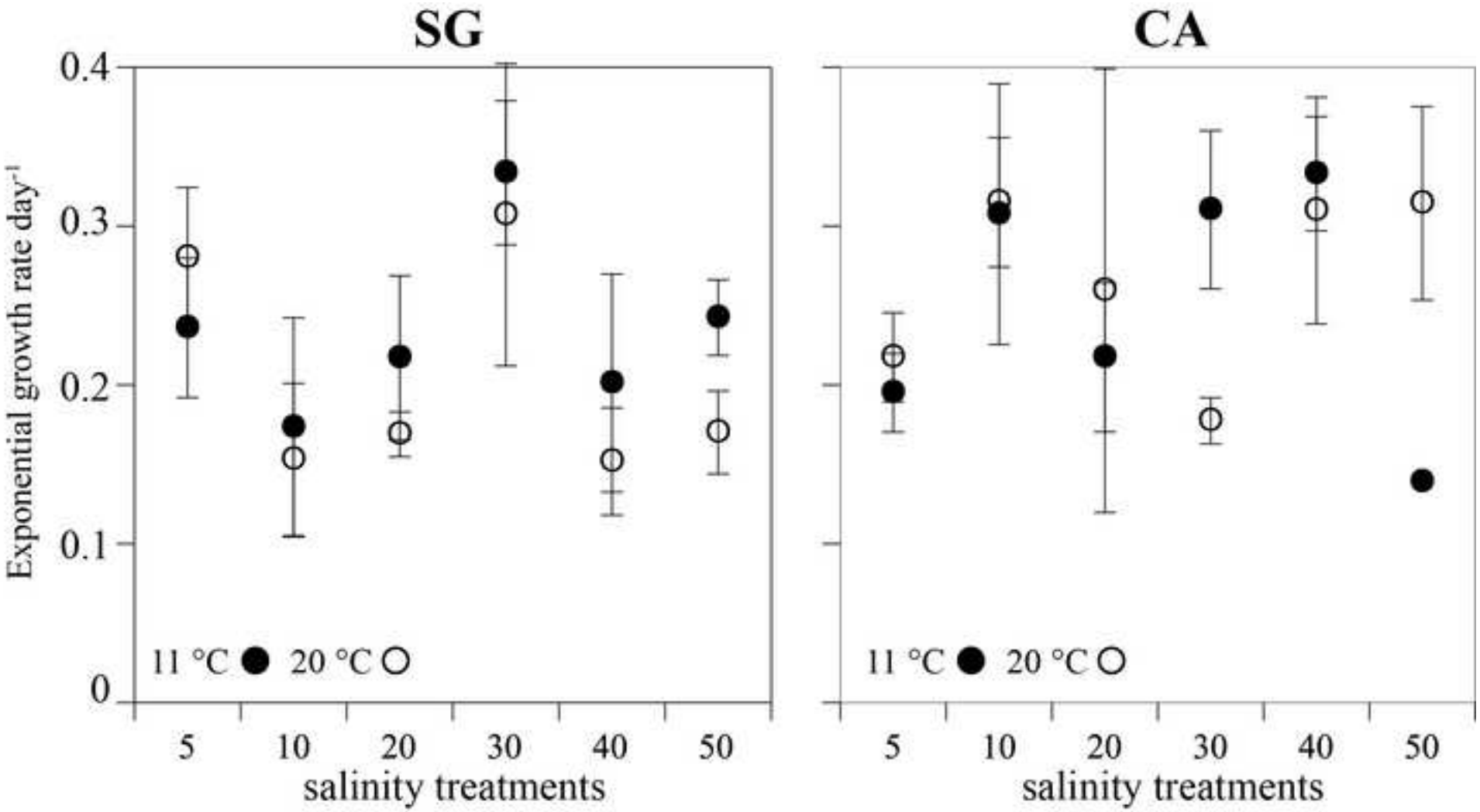

Table 1 *Kryptoperidinium* monthly mean cell density, maximum cell density and frequency of species observations in each month (±standard deviation and number of records) in Santa Giusta (SG) and Calich (CA) lagoons. Monthly means derived from data obtained in each month in the study periods (May 2011 to September 2016 for SG and from September 2008 to June 2015 for CA).

	Mean cell density (cells x 10^4 L)		**Max cell density** (cells x 10^4 L)		**Frequency obs.** (%)	
	SG	**CA**	**SG**	**CA**	**SG**	**CA**
Jan	0 (-)	6.74 (±14.5; 6)	-	36.14	-	50
Feb	0.05 (±0.6; 7)	8.60 (±12.8; 9)	0.12	38.73	57	67
Mar	0 (-)	13.97 (±46.2; 18)	-	195.05	-	33
Apr	0 (-)	57.21 (±113.2; 15)	-	422.51	-	67
May	0 (-)	4.14 (±5.5; 15)	-	16.95	-	67
Jun	0 (-)	7.07 (±8.9; 15)	-	29.35	-	80
Jul	5.29 (±14.5; 27)	7.71 (±21.7; 12)	63.54	75.84	15	33
Aug	0.13 (±0.5; 27)	3.82 (±12.3; 12)	2.09	42.71	7	25
Sep	0 (-)	0 (-)	-	-	-	-
Oct	0 (-)	0.13 (±0.3; 12)	-	1.04	-	17
Nov	0 (-)	4.87 (±12.4; 15)	-	35.88	-	27
Dec	0 (-)	3.05 (±8.8; 15)	-	33.77	-	33

Table 2

Table 2 Monthly mean values (±standard deviation and number of records) of dissolved inorganic nitrogen (DIN), reactive phosphorous (PO_4), DIN and PO_4 ratio in Santa Giusta (SG) and Calich (CA) lagoons. Monthly means derived from data obtained in the entire study period for each month (May 2011 to September 2016 for SG and from September 2008 to June 2015 for CA).

		Jan	**Feb**	**Mar**	**Apr**	**May**	**Jun**	**Jul**	**Aug**	**Sep**	**Oct**	**Nov**	**Dec**	**Annual Mean**
DIN (µM)	SG	5.55 (±4.8; 11)	3.38 (±1.6; 7)	5.94 (±5.6; 12)	1.45 (±0.7; 15)	3.40 (±2.7; 16)	1.56 (±1.0; 28)	4.95 (±7.4; 27)	3.80 (±6.1; 27)	2.06 (±1.3; 24)	2.57 (±2.3; 20)	7.17 (±6.4; 15)	12.06 (±15.4; 15)	4.49
	CA	124.22 (±72.9; 6)	96.93 (±54.7; 9)	117.72 (±57.2; 18)	72.02 (±53.9; 15)	46.98 (±27.9; 15)	9.37 (±9.7; 15)	7.07 (±7.1; 12)	6.52 (±7.4; 12)	18.51 (±19.1; 15)	27.78 (±16.7; 12)	65.14 (±38.9; 16)	158.46 (±64.0; 16)	62.56
PO_4 (µM)	SG	0.72 (±1.2; 11)	0.38 (±0.4; 7)	1.32 (±0.5; 12)	0.69 (±0.4; 15)	0.68 (±0.6; 16)	0.48 (±0.6; 28)	0.31 (±0.2; 27)	0.33 (±0.2; 27)	0.33 (±0.2; 24)	0.33 (±0.3; 20)	0.68 (±0.6; 15)	1.12 (±0.8; 15)	0.61
	CA	3.58 (±1.4; 6)	2.24 (±0.8; 9)	2.07 (±1.7; 18)	3.37 (±2.7; 15)	2.54 (±2.1; 15)	1.83 (±2.2; 15)	0.81 (±0.9;1 12)	1.33 (±1.5; 12)	4.89 (±6.7; 15)	2.22 (±2.7; 12)	5.39 (±4.8; 16)	5.72 (±3.7; 16)	3.00
DIN: PO_4	SG	37.40 (±48.0; 11)	18.28 (±28.2; 7)	3.83 (±2.5; 12)	3.51 (±3.3; 15)	9.51 (±9.1; 16)	8.69 (±15.2; 28)	24.34 (±46.0; 27)	22.67 (±44.4; 27)	12.39 (±14.1; 24)	13.45 (±14.1; 20)	13.76 (±8.6; 15)	9.32 (±6.2; 15)	14.76
	CA	32.91 (±11.5; 6)	76.38 (±107.5; 9)	142.66 (±214.5; 18)	81.09 (±183.4; 15)	148.24 (±279.8; 15)	21.20 (±32.1; 15)	14.90 (±20.1; 12)	9.51 (±13.2; 12)	17.94 (±20.9; 15)	112.76 (±179.9; 12)	25.63 (±21.7; 16)	33.04 (±15.1; 16)	59.69

Table 3 Synthesis of the results of the generalized linear models (GLMs) applied on the absence/presence data of *Kryptoperidinium* and on selected environmental variables using the Calich Lagoon (CA) and Santa Giusta Lagoon (SG) set of data and the entire set of data (CA plus SG data). GLM was also applied to two different thresholds of *Kryptoperidinium* cell density: 1) >2 x 10^5 cells L^{-1}; 2) >3 x 10^5 cells L^{-1}. Significant effects are shown in bold.

GLM - **CA DATA** absence/presence				
	Estimate	Standard error	*Z* value	Pr (>*Z*)
(Intercept)	0.474	0.775	0.611	0.541
Sal	−0.016	0.025	−0.639	0.523
DIN	0.007	0.004	2.129	**0.033**
PO_4	−0.004	0.051	−0.082	0.935
Rain	−0.011	0.004	−2.817	**0.005**

GLM - **SG DATA** absence/presence				
	Estimate	Standard error	*Z* value	Pr (>*Z*)
(Intercept)	−7.693	2.809	−2.739	**0.006**
Sal	0.107	0.069	1.551	0.121
DIN	0.114	0.038	3.028	**0.002**
Rain	0.08	0.011	0.722	0.470

GLM - **CA plus SG DATA** absence/presence				
	Estimate	Standard error	*Z* value	Pr (>*Z*)
(Intercept)	0.338	0.649	0.521	0.603
Sal	−0.065	0.019	−3.429	**0.000**
DIN	0.009	0.003	2.783	**0.005**
Rain	−0.007	0.004	−2.043	**0.041**

Figure Suppl 1

Figure Suppl 2

English revision certificate

HARMFUL ALGAE

AUTHOR DECLARATION

Submission of an article implies that the work described has not been published previously (except in the form of an abstract or as part of a published lecture or academic thesis), that it is not under consideration for publication elsewhere, that its publication is approved by all authors and tacitly or explicitly by the responsible authorities where the work was carried out, and that, if accepted, it will not be published elsewhere in the same form, in English or in any other language, without the written consent of the copyright-holder.

By attaching this Declaration to the submission, the corresponding author certifies that:

- The manuscript represents original and valid work and that neither this manuscript nor one with substantially similar content under the same authorship has been published or is being considered for publication elsewhere.

- Every author has agreed to allow the corresponding author to serve as the primary correspondent with the editorial office, and to review the edited typescript and proof.

- Each author has given final approval of the submitted manuscript and order of authors. Any subsequent change to authorship will be approved by all authors.

- Each author has participated sufficiently in the work to take public responsibility for all the content.

*Declaration of Interest Statement

Declaration of interests

X The authors declare that they have no known competing financial interests or personal relationships that could have appeared to influence the work reported in this paper.

☐The authors declare the following financial interests/personal relationships which may be considered as potential competing interests: